

TOTEM: TOKENIZED TIME SERIES EMBEDDINGS for General Time Series Analysis

Anonymous authors
Paper under double-blind review

Abstract

This work studies the problem of time series analysis with *generalist* models, or models trained across many data domains. Drawing inspiration from the widespread success of large language models, we consider the simple strategy of discretely tokenizing time series data drawn from a myriad of datasets via self-supervision, then using the fixed tokenization to solve a variety of tasks across many data domains. Canonically time series models are either trained on a single dataset, or built in a task specific manner (e.g. only a forecaster), or use patches of time as inputs to the model. As such, performant generalist, multi-task, discrete representation time series models are of value. Our method, TOKENIZED TIME SERIES EMBEDDINGS (TOTEM), produces such generalist time series models with minimal or no fine-tuning, while exhibiting strong zero-shot performance. We evaluate TOTEM extensively over nearly 500 experiments on three commonly-studied time series tasks with real-world data: imputation (17 baselines, 12 datasets), anomaly detection (19 baselines, 25 datasets), and forecasting (14 baselines, 12 datasets). We conclude that TOTEM matches or outperforms existing state-of-the-art models in both the canonical specialist setting (i.e., training one model on one domain) as well as the generalist setting (i.e., training a single model on many domains), which demonstrates the efficacy of tokenization for general time series analysis.

1 Introduction

We study generalist time series models with unified discrete data representations across many tasks. *Generalist models* are trained on many data domains simultaneously, which contrasts *specialist models* that are trained on a single time series domain Zhou et al. (2023); Wu et al. (2022a); Nie et al. (2022), Figure 1A.

Time series analysis has typically been restricted by task, where methods study only *imputation* Luo et al. (2018; 2019); Talukder et al. (2022), or *anomaly detection* Xu et al. (2021); He & Zhao (2019), or *forecasting* Wu et al. (2021); Woo et al. (2022) among others. Recently, the field has become increasingly unified with respect to model architecture, with methods Zhou et al. (2023); Wu et al. (2022a) exploring language and vision backbones on various time series tasks. These backbones, like previous methods, utilize specialist training (e.g., training separate imputers on each dataset).

Time series analysis has also become increasingly unified with respect to data representations (Yue et al., 2022; Yang & Hong, 2022; Tonekaboni et al., 2021; Franceschi et al., 2019), some of which are discrete (Lin et al., 2007; Van Den Oord et al., 2017; Baevski et al., 2020; Rabanser et al., 2020). Unified discrete data representations, both statistical and learnt, have been more extensively studied in language and vision modeling (Gage, 1994; Van Den Oord et al., 2017; Esser et al., 2021; Rombach et al., 2022).

When considering model evaluation, both specialist and generalist models can be tested under various regimes. Within *in-domain-testing*, a model is tested on the same domain(s) it was trained on. In *zero-shot-testing*, a model is tested on different domains(s) than it was trained on, Figure 1B. Most time series methods are evaluated via in-domain-testing. Some methods have begun to explore the idea of zero-shot forecasting where (1) a forecaster trains on one dataset then predicts on a separate dataset (Zhou et al., 2023), or (2) a forecaster trains on a subset of channels (which we call *sensors*) from one dataset then zero-shot forecasts on the remaining sensors in the same dataset (Liu et al., 2023). However, both of these models would be

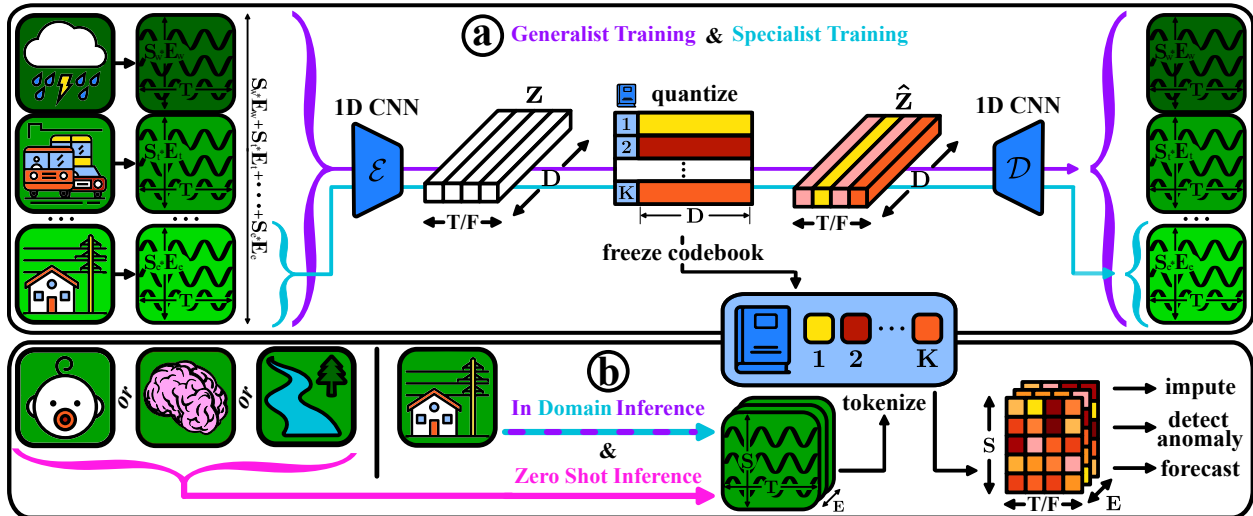


Figure 1: **TOTEM Overview, Training Schemas, Inference Regimes & Tasks.** (a) TOTEM’s VQVAE enables **generalist training**, *i.e.*, on many data domains jointly, and **specialist training**, *i.e.*, on one data domain at a time. The TOTEM VQVAE architecture consists of an 1D strided CNN encoder \mathcal{E} , quantizer, latent codebook, and 1D strided transpose CNN decoder \mathcal{D} . (b) TOTEM’s discrete, self-supervised codebook is frozen then leveraged for both **in domain** and **zero shot** testing across many tasks.

considered specialists, as they were trained on only one (or a subset of one) dataset. In this paper we move beyond specialist zero-shot forecasting and extensively study zero-shot performance in generalist models across multiple tasks.

Our approach to studying what is a performant general time series data representation shares a philosophical alignment with the development of large generalist models in natural language processing, which are also based on having a common tokenized representation Gage (1994); Radford et al. (2018). Through extensive evaluations we find that a good discrete token representation is a key building block for performant generalist models with strong zero shot performance. Leveraging 17 baselines and 12 datasets in imputation, 19 baselines and 25 datasets in anomaly detection, and 14 baselines and 12 datasets in forecasting we evaluate TOTEM in the (1) standard specialist regime and (2) generalist regime with both in-domain and zero shot testing. In the specialist setting, TOTEM matches or outperforms SOTA when compared to many heavily customized task-specific models, despite the fact that TOTEM has minimal to no tuning. In the generalist setting, TOTEM also matches or outperforms SOTA. Our contributions include (1) providing a simple yet performant implementation amongst a vast technical landscape, specifically a single vector quantized variational autoencoder architecture that can be applied to a variety of tasks and data domains with minimal or no tuning, for generalist and specialist imputers, anomaly detectors, and forecasters, and (2) performing an exhaustive evaluation across tasks (imputation, anomaly detection, forecasting), model categories (specialist, generalist), evaluation schemas (in-domain, zero-shot), baselines (17 imputation, 19 anomaly detection, 14 forecasting), and real world datasets (12 imputation, 25 anomaly detection, 12 forecasting) resulting in nearly 500 experiments.

2 Related Work

Time series modeling methods utilize many techniques, ranging from statistical methods Winters (1960); Holt (1957); Anderson (1976); Hyndman & Athanasopoulos (2018); Taylor & Letham (2018) to multilayer perceptrons (MLPs) Zeng et al. (2023); Li et al. (2023); Das et al. (2023a); Challu et al. (2023); Chen et al. (2023); Zhang et al. (2022); Oreshkin et al. (2019) to convolutional neural networks (CNNs) Wu et al. (2022a); Liu et al. (2022a); He & Zhao (2019); Franceschi et al. (2019); Bai et al. (2018) to recurrent neural networks (RNNs) Salinas et al. (2020); Shen et al. (2020); Hochreiter & Schmidhuber (1997) to transformers Zhou et al. (2023); Liu et al. (2023); Nie et al. (2022); Zhang & Yan (2022); Woo et al. (2022); Zhou et al. (2022); Liu et al.

(2022b); Wu et al. (2022b); Xu et al. (2021); Wu et al. (2021); Liu et al. (2021); Zhou et al. (2021); Kitaev et al. (2020); Li et al. (2019). Many models are hybrid solutions that blend aforementioned approaches.

Most of these methods intake time and then perform various combinations of normalization (Kim et al., 2021), frequency transformations (Wu et al., 2022a; Zhou et al., 2022), and patchification (Nie et al., 2022). Time and sensor patch dependencies are then learned, via an attention mechanism, convolution, recurrence, or linear layer, across the temporal dimension, sensor dimension, or both the temporal and sensor dimensions (Zhang & Yan, 2022). For multisensor modeling, one can model all sensors jointly or independently (i.e., forecast each sensor independently (Nie et al., 2022)).

The time series community has long valued discrete data representations (Baeviski et al., 2020; Rabanser et al., 2020; Oord et al., 2016; Lin et al., 2007), unified data representations Yang & Hong (2022); Yue et al. (2022); Tonekaboni et al. (2021); Barnum et al. (2020); Franceschi et al. (2019), and models’ performance on multiple tasks (Zhou et al., 2023; Wu et al., 2022a; Lin et al., 2007). Additionally, since the success of large language and vision models, work concurrent or subsequent to our own has begun to focus on generalist training, where models are trained on multiple domains at once (Das et al., 2023b; Ansari et al., 2024; Goswami et al., 2024). In the following sections we further discuss generalist training, discrete data representations, and tasks.

Specialist vs Generalist Training. Historically, specialist training, where models are only trained on a single time series domain, has been the most common amongst prior work (Zhou et al., 2023; Wu et al., 2022a; Nie et al., 2022; Zhang & Yan, 2022). These specialist models are primarily evaluated via in-domain-testing, where the test set is from the same domain as the train set. Recently, some methods (Zhou et al., 2023; Liu et al., 2023) have begun to explore specialist zero-shot forecasting capabilities. Generalist training, where models are trained on multiple domains at once (e.g. weather, traffic, and electricity), is an emerging regime that concurrent and subsequent work to our own have begun to adopt (Das et al., 2023b; Ansari et al., 2024; Goswami et al., 2024). However, unlike TOTEM (Ours), none of these methods explore all three dimensions of generalist training, discrete tokenization, and multiple tasks, see Table 1.

Patches vs Discrete Data Representations. Much prior work does not leverage discrete data representations for time series, instead relying on patchification either along the time dimension (Liu et al., 2023; Zhang & Yan, 2022; Nie et al., 2022), or sensor dimension Li et al. (2019); Zhou et al. (2021); Wu et al. (2021); Liu et al. (2021)¹. Patches are simply chunks of time. Patch lengths range from a single time-step/sensor, also known as point-wise, to the length of the entire time series/all sensors. These methods learn the underlying data representations end-to-end with the downstream task (e.g., forecasting). Prior work that leverages discrete data representations study varying methods including product quantization (Baeviski et al., 2020), binning (Rabanser et al., 2020), symbolic representations (Lin et al., 2007), and vector quantization (Van Den Oord et al., 2017). Unlike TOTEM (Ours), none of these methods explore all three dimensions of generalist training, discrete tokenization, and multiple tasks, see Table 1.

Discrete unified representations, both statistical and learnt, have been more extensively studied in language and vision modeling (Gage, 1994; Van Den Oord et al., 2017; Esser et al., 2021; Rombach et al., 2022). The vision modeling field distinguishes between discrete, learnt, tokens (Van Den Oord et al., 2017; Esser et al., 2021; Rombach et al., 2022) and patches (Dosovitskiy et al., 2020). Patches have been extensively studied in modern time series modeling (Zhou et al., 2023; Nie et al., 2022; Zhang & Yan, 2022). Given the success of vector quantized variational autoencoders (VQVAEs) in both the audio and vision domains (Van Den Oord et al., 2017; Esser et al., 2021; Rombach et al., 2022), we utilize the VQVAE to create discrete tokens for general time series analysis across multiple tasks. TOTEM’s representation is independent of the downstream model, similar to byte pair encoding in large language modeling (Gage, 1994; Radford et al., 2018).

Time Series Tasks. In time series analysis there are many tasks: such as forecasting (with both long term and short term horizons), anomaly detection, imputation, and classification. Most prior work focuses on a single task (Zhang & Yan, 2022; Nie et al., 2022; Xu et al., 2021), with a few exploring multiple specialist trained models on many tasks (Zhou et al., 2023; Wu et al., 2022a). Concurrent and subsequent work is also mainly focused on single task models (Ansari et al., 2024; Das et al., 2023b), with fewer focusing on multiple

¹In time series analysis, sensors, channels, and variates are synonymous terms; in this paper we adopt the sensor terminology.

tasks (Goswami et al., 2024). Unlike TOTEM (Ours), none of these methods study all three dimensions of generalist training, discrete tokenization, and multiple tasks, see Table 1.

The long term forecasting task uses standardized input-to-output dimensionalities consistent across datasets. An input dimension of 96 and output dimensions of 96, 192, 336, and 720 is the standard enforced by Liu et al. (2023); Wu et al. (2022a); Liu et al. (2022b); Zhou et al. (2022) among others². Our method, TOTEM, follows this standard. On the other hand, short term forecasting has highly non-standard and dataset-specific input-to-output dimensionalities (see Table 15), and this lack of standardization impedes generalist training (one model trained over many domains)³. In classification and anomaly detection, many modern baselines are leaky (Zhou et al., 2023; Wu et al., 2022a; Xu et al., 2021), where leakage is defined as using the test set in the training and validation process. We felt strongly about not propagating leaky SOTA results, because that further promotes faulty baselines. In classification others have already built off of TOTEM and demonstrated SOTA performance for neural decoding utilizing clean datasets and non-leaky practices (Chau et al., 2024). In anomaly detection we were able to establish TOTEM as a non-leaky SOTA baseline, even when comparing against leaky baselines. Beyond the leaky training setup, the canonical anomaly detection benchmark datasets used by (Zhou et al., 2023; Wu et al., 2022a; Xu et al., 2021) are additionally flawed (Wu & Keogh, 2021). Therefore we include the flawed benchmarks to enable comparison to prior work 5, 6, 7 and also included comparisons to 15 unflawed benchmarks 9 from Wu & Keogh (2021) in the Appendix. Given the considerations towards building generalist models, not propagating leaky baselines, and utilizing clean datasets while still enabling prior comparisons, we study long term forecasting (henceforth referred to as forecasting), imputation, and anomaly detection in this paper.

	Generalist Training	Discrete Tokenization	Multiple Tasks
Prior	GPT2 (Zhou et al., 2023)	✗	✗
	TiNet (Wu et al., 2022a)	✗	✗
	W2V2.0 (Baevski et al., 2020)	✗	✓
	SAX (Lin et al., 2007)	✗	✓
C/S	TimesFM (Das et al., 2023b)	✓	✗
	Chronos (Ansari et al., 2024)	✓	✗
	MNT (Goswami et al., 2024)	✓	✓
	TOTEM (Ours)	✓	✓

Table 1: **Related Work Overview.** TOTEM (Ours) explores all three dimensions of generalist training, discrete tokenization, and multiple tasks unlike prior and much concurrent/subsequent (C/S) work. Generalist training is training on multiple data domains at once; discrete tokenization is using a fixed number of representations; multiple tasks is studying numerous tasks, e.g. imputation, anomaly detection & forecasting.

3 Method

3.1 Design Decisions

When designing the TOTEM training and testing stack to enable generalist-training and zero-shot testing across many tasks there were three important design decisions to consider (1) two stage learning, (2) operating across the time dimension, and (3) no data engineering.

Two Stage Learning. We learn a tokenizer, Figure 1a, independently from a downstream model (e.g. forecaster), Figure 1b and Figure 4. This design decision enables exploration of (1) downstream architectures with fixed representations and (2) zero shot capabilities with data scale and diversity. When exploring (1) the value of differing downstream architectures, we utilize either a transformer encoder or MLP, Table 17A &

²Some methods utilize a 512 input dimension, which make consistent comparisons challenging; despite this field-wide inconsistency we include some of these results in the Appendix 16. TOTEM (Ours) outperforms other methods across lookback lengths 96, 512 at 58.3% AvgWins, the next best is GPT2 at 8.3% AvgWins.

³Despite this we demonstrate that TOTEM and GPT2 outperform all other methods on a subset of short term forecasting lengths and datasets in the Appendix 14.

E. It is important for these models to pull from the same representation as the two stage learning framework disentangles modeling a data representation from modeling interactions across time, unlike end-to-end learnt representations. This is significant as much modern time series literature (Ekambaram et al., 2023; Das et al., 2023a; Zeng et al., 2023) questions the value of transformers when compared to MLPs. Ultimately studying which architecture is suited to which function, e.g. representing or learning interactions, is valuable to the community. We leave in-depth analysis on the merits of transformers versus MLPs to future work, but note that discrete tokens lead to better performance when compared to patches for both model types: transformer (67.9% to 39.3% **AvgWins**) and MLP (66.1% to 37.5% **AvgWins**), Figure 8. When exploring (2) zero shot capabilities with data scale and diversity we take inspiration from large language models. In large language models a byte-pair-encoding (BPE) Gage (1994); Radford et al. (2018) representation is calculated on large amounts of diverse data before downstream modeling. At test time unseen data can be successfully represented by these pre-calculated BPE tokens and then fed into the pre-trained downstream model for zero-shot performance. In language modeling, this two-step represent then solve-task process has been wildly successful as training data quantity and diversity increases. Indeed, in our experiments on time series, we find that as we increase data scale and diversity TOTEM performs better on zero-shot datasets, Figure 11 & Table 21. We believe that as we further scale the number of diverse training time series TOTEM could create powerful fixed representations that accurately represent a wide array of domains that, significantly, do not need to be recalculated when representing new domains, akin to BPE for language modeling.

Operating Across the Time Dimension. A time series dataset consists of E examples (i.e. number of distinct recordings), S sensor channels, and T time steps, and can be formally expressed as $\{\mathbf{x}_j\}_{j=1}^E \subset \mathbb{R}^{S \times T}$. Prior work commonly patches (not tokenizes) along either the sensor dimension Li et al. (2019); Zhou et al. (2021); Wu et al. (2021); Liu et al. (2021), or time dimension Liu et al. (2023); Zhang & Yan (2022); Nie et al. (2022). When considering specialist trained models and in-domain testing, e.g. an electricity forecaster where the train and test sets are derived from the same dataset, tokenization can be applied across any dimension E , S , or T , Figure 2 left. However when moving to either generalist trained models, e.g. a forecaster trained on electricity and traffic and weather domains whose S and E dimensions all differ, or the zero-shot testing regime, e.g. testing on domains which can have differing S and E dimensions, operating along the time dimension is necessary, Figure 2 right. Our tokenizer handles varying dimensionality across E , S , and T by creating discrete non-overlapping tokens along the time-dimension of length F , where $F < T$, thereby promoting training and testing on variable length examples, E , sensors, S , and time steps T . This design decision enables generalist training and zero shot testing.

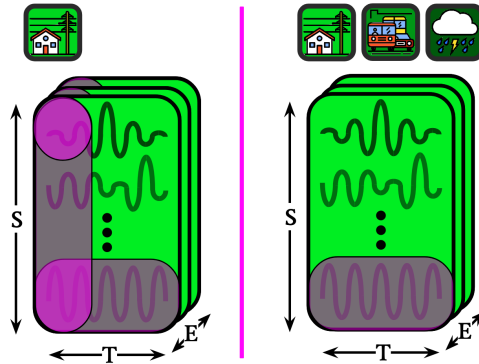


Figure 2: **Specialist vs. Generalist Potential Tokenization Dimensions.** Left, with specialist models tested via in-domain testing, tokenization can be applied along E , S , or T . Right, with either generalist models or zero-shot testing tokenization should be applied along T .

No Data Engineering. Most prior work leverages normalization, and we do not consider this to be data engineering. Manipulations in prior work that we do consider to be data engineering include the use of auxiliary features (e.g. day of the month, or minute in the hour, etc.) Chen et al. (2023); Salinas et al. (2020), or frequency transformations Wu et al. (2022a); Zhou et al. (2022). We forego any data engineering and operate directly on time steps. This enables generalist training and zero shot testing as differing data domains have widely varying sampling rates, Table 3, leading to distinct auxiliary features and frequency profiles.

3.2 Task Definitions

There are numerous tasks to tackle in time series analysis. Three significant ones are imputation, anomaly detection, and forecasting. In *imputation*, models intake a masked time series $\mathbf{x}_m \in \mathbb{R}^{S \times T_{in}}$, and then reconstruct and impute $\mathbf{x} \in \mathbb{R}^{S \times T_{in}}$. In *anomaly detection*, models intake a corrupted time series $\mathbf{x}_{corr} \in \mathbb{R}^{S \times T_{in}}$ and reconstruct the data $\mathbf{x} \in \mathbb{R}^{S \times T_{in}}$. The amount of corruption is considered known, at $A\%$. In *forecasting*, models intake a time series $\mathbf{x} \in \mathbb{R}^{S \times T_{in}}$ and predict future readings $\mathbf{y} \in \mathbb{R}^{S \times T_{out}}$, where S is the

number of sensors and $T_{\text{in}}, T_{\text{out}}$ signify the durations of the preceding and succeeding time series, respectively. When implementing a tokenizer, it should be performant across all tasks despite their distinct representational requirements with minimal to no tuning while maintaining the same architecture and objective regardless of the downstream task.

3.3 Tokenizer Implementation

To realize a single tokenizer architecture that enables generalist modeling across differing domains and tasks we take inspiration from the VQVAE (Van Den Oord et al., 2017). The original VQVAE leverages a dilated convolutional architecture with a stride of 2 and window-size of 4, similar to the WaveNet (Oord et al., 2016) dilated, causal, convolutional decoder. A dilated convolution skips inputs allowing a filter to operate on a larger input area / coarser scale. Utilizing dilated convolutions is an architectural decision rooted in the high sampling rates of raw audio waveforms (Oord et al., 2016; Van Den Oord et al., 2017). High sampling rates are not a trait shared by many time series domains, Table 3. When training the tokenizer we stride all input data by 1 time step, while keeping a long (e.g. 96 time steps) input. This enables the tokenizer to see every possible combination of time when learning a discrete number of codewords to represent the training set while enabling a large receptive field, see Figure 14 for codebook visualizations. Finally the tokenizer can also learn codewords in a normalized space, Figure 3. This enables the codewords to represent normalized waveforms instead of taking both scale and waveform into account. Scale (mean and std. dev.) can be returned in the downstream modeling, see Figure 4 if needed for the task. Using a strided non-causal convolutional architecture with no dilation, pre-striding the data by 1, training on long time series inputs, and enabling the separation between scale and waveform allows the tokenizer to capture maximal information within a large receptive field.

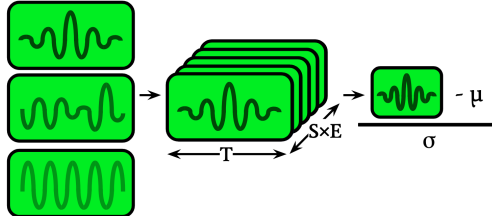


Figure 3: TOTEM flattens the sensor dimension, S , and example dimension, E , into the batch and learns a discrete representation along the time dimension, T . Tokens can be learnt in a normalized space.

The TOTEM VQVAE consists of an encoder, quantizer, latent codebook, and decoder. It takes in a univariate time series $\{\mathbf{x}_i \in \mathbb{R}^T\}_{i=1}^{E \cdot S}$ obtained by flattening the sensor channel of the multivariate data, Figure 3. This makes TOTEM’s VQVAE sensor-agnostic, enabling TOTEM’s generalist-training and zero-shot-testing. The encoder \mathcal{E} consists of strided 1D convolutions compressing the time series by a cumulative stride of F . \mathcal{E} maps a univariate time series $\mathbf{x} \in \mathbb{R}^T$ to a latent representation $\mathbf{z} = \mathcal{E}(\mathbf{x}) \in \mathbb{R}^{T/F \times D}$, where D is the the hidden dimension. The latent codebook $\mathcal{C} = \{\mathbf{c}_i\}_{i=1}^K$ consists of K D -dim codewords $\mathbf{c}_i \in \mathbb{R}^D$. During quantization, the codebook is used to replace \mathbf{z} with $\hat{\mathbf{z}} \in \mathbb{R}^{T/F \times D}$ such that $\hat{\mathbf{z}}_j = \mathbf{c}_k$, where $k = \arg \min_i \|\mathbf{z}_j - \mathbf{c}_i\|_2$. The decoder \mathcal{D} follows the reverse architecture of the encoder \mathcal{E} , consisting of 1D transpose convolutions with a cumulative stride of $1/F$ mapping the quantized $\hat{\mathbf{z}}$ to a reconstructed time series $\hat{\mathbf{x}} = \mathcal{D}(\hat{\mathbf{z}}) \in \mathbb{R}^T$. We exclusively use a compression factor of $F = 4$, Table 25. We learn \mathcal{E} , \mathcal{D} , and \mathcal{C} by optimizing the objective $\mathcal{L} = \mathcal{L}_{\text{rec}} + \mathcal{L}_{\text{cmt}}$ consisting of a reconstruction loss $\mathcal{L}_{\text{rec}} = \frac{1}{E \cdot S} \sum_i \|\mathbf{x}_i - \hat{\mathbf{x}}_i\|_2^2$ and a commitment loss \mathcal{L}_{cmt} , which follows a similar formulation but allows the codebook to update despite the the non-differentiable arg min operation during quantization. Notably, this objective does not change even when the underlying task, time series length, data masking, normalization schema, or data domain changes. See §A.9 & §A.10 for additional details.

3.4 Downstream Model Implementation

Notably imputation and anomaly detection can be directly solved with just TOTEM’s VQVAE, see Figures 12 and 13, as they are fundamentally data representation tasks, whereas in forecasting further modeling is required, see Figure 4. In forecasting, the trained, frozen, codebook representation converts a sensor’s observed measurements $\mathbf{x}_s \in \mathbb{R}^{T_{\text{in}}}$ to a sequence of T_{in}/F discrete tokens. The forecaster transformer encoder processes these tokenized time series independently for each sensor, adding time-based positional encodings to each token along the time dimension. Using a series of multi-head attention layers, the model predicts the forecasted measurements $\bar{\mathbf{y}}_s \in \mathbb{R}^{T_{\text{out}}}$ for $s = 1, \dots, S$, applying the attention mechanism along the time dimension T . In parallel, the forecaster takes in \mathbf{x}_s and predicts the future’s mean, μ_s , and standard deviation, σ_s , for each sensor $s = 1, \dots, S$ to unnormalize the data. The final forecasted prediction is $\mathbf{y}_s = \sigma_s \cdot \bar{\mathbf{y}}_s + \mu_s$.

The forecaster is trained in a supervised fashion by minimizing three smooth L1 losses between predictions $\{\bar{y}_s, \mu_s, \sigma_s\}$ and their ground truth respectively.

Our proposed two-step discrete time series tokenization then modeling framework enables the design of general models across a variety of time series domains, tasks, and evaluation schemas, Figure 1. We design a single tokenizer architecture that is generally applicable without extensive data engineering while being suitable for varying data dimensionalities across different tasks. There are many possibilities for how to introduce a discrete time series tokenizer, we extensively study one such methodology that maintains the same architecture and objective regardless of the downstream task and satisfies the aforementioned design criteria. See §A.9 & §A.10 for additional details.

4 Experimental Setup

4.1 Imputation.

Baselines. For the specialist setting, we compare against 11 baselines spanning linear models, transformers, and convolutional neural networks. These eleven include two recent models that explore multiple tasks, the transformer based GPT2 (Zhou et al., 2023) and the convolutional TimesNet [TiNet] (Wu et al., 2022a). For models which were only designed for a single task we compare against PatchTST [Patch] (Nie et al., 2022), ETSFormer [ETS] (Woo et al., 2022), Fedformer [FED] (Zhou et al., 2022), Non-stationary trans. [Stat] (Liu et al., 2022b), Autoformer [Auto] (Wu et al., 2021), Informer [Inf] (Zhou et al., 2021), Reformer [Re] (Kitaev et al., 2020), LightTS [LiTS] (Zhang et al., 2022), DLinear [DLin] (Zeng et al., 2023). We pull these values from (Zhou et al., 2023). Additionally in the Appendix, Table 5, we compare to 5 additional baselines spanning variational autoencoders, recurrent neural networks, and score-based diffusion models: V-Rin(Mulyadi et al., 2021), BRITS(Cao et al., 2018), RDIS(Choi et al., 2023), unconditional and CSDI(Tashiro et al., 2021). These values are taken from (Tashiro et al., 2021). We also setup GPT2 (Zhou et al., 2023) to run in a generalist manner. *In total we use or train 17 imputation baselines.* **Datasets.** We evaluate on 6 benchmark datasets: weather [W], electricity [E], ETTm1 [m1], ETTm2 [m2], ETTh1 [h1], ETTh2 [h2], which are most recently used by Zhou et al. (2023). For the zero shot settings, we use 5 benchmark datasets: neuro2 [N2], neuro5 [N5] Peterson et al. (2022), and saugeen river flow [R], U.S. births [B], and sunspot [S] Godahewa et al. (2021). Additionally in the Appendix, Table 5, we utilize the PhysioNet Challenge 2012 dataset (Silva et al., 2012). *In total we use 12 datasets for imputation.* **Metrics.** Consistent with prior work, we report mean squared error MSE (lower is better \downarrow), mean absolute error MAE (\downarrow).

4.2 Anomaly Detection.

Baselines. For the specialist setting, we compare against 15 baselines spanning linear models, transformers, and convolutional neural networks; namely: GPT2, TiNet, Anomaly trans. [ATran](Xu et al., 2021), Patch, ETS, FED, Stat, Auto, Pyraformer [Pyra] (Liu et al., 2021), Inf, Re, LogTrans. [LogTr] (Li et al., 2019), Trans. [Trans] (Vaswani et al., 2017), LiTS, and DLin. These values come from (Zhou et al., 2023). Additionally in the Appendix, Table 9, we compare to 3 additional baselines DGHL (Challu et al., 2022) and work that is concurrent/subsequent to our own MNT-0, and MNT-LP(Goswami et al., 2024). These values come from (Goswami et al., 2024). We also setup GPT2 (Zhou et al., 2023) to run in a generalist manner. *In total we use or train 19 anomaly detection baselines.* **Datasets.** We leverage 5 recent(Zhou et al., 2023) SMD, MSL, SMAP, SWAT, PSM anomaly detection datasets, as well as 5 datasets for zero shot: neuro2 [N2], neuro5 [N5]

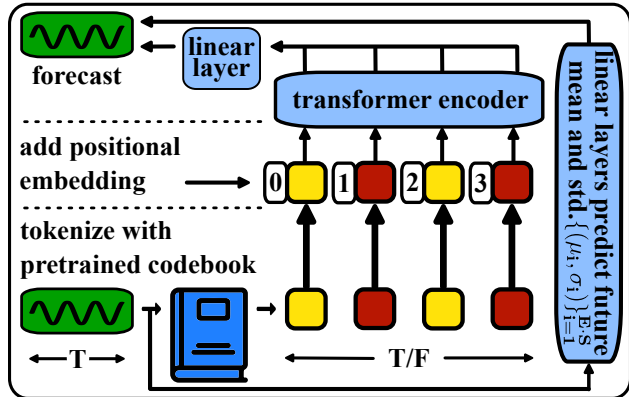


Figure 4: **Forecaster Modeling.** The forecasting task requires modeling beyond the VQVAE. We leverage TOTEM’s pretrained, learnt, discrete codes as the input data representation and train a transformer encoder. We add positional embeddings along the time dimension, and use linear layers before the final output as well as to un-normalize the resulting forecast.

Peterson et al. (2022), and saugeen river flow [R], U.S. births [B], and sunspot [S] Godahewa et al. (2021). In the Appendix, Table 9, we also use 15 dataset from (Wu & Keogh, 2021). *In total we use 25 datasets for anomaly detection.* **Metrics.** Consistent with prior work, we report precision P (higher is better \uparrow), recall R (\uparrow), and adjusted F1 score (\uparrow).

4.3 Forecasting.

Baselines. For the specialist setting, we compare against 11 baselines spanning linear models, transformers, and convolutional neural networks: GPT2, TiNet, iTrans. [iTrans] Liu et al. (2023), Patch, Crossformer [Cross] Zhang & Yan (2022), FED, Stat, TiDE Das et al. (2023a), RLinear [RLin] Li et al. (2023), DLin, and SciNet [SCi] Liu et al. (2022a). We run GPT2 with a lookback length of 96 as they originally report varying, dataset-specific, lookback lengths. Numbers for other methods are from (Liu et al., 2023). In the Appendix, Table 16, we additionally compare to N-Beats(Oreshkin et al., 2019) and work that is concurrent/subsequent to our own MNT (Goswami et al., 2024). Additionally, we implement the GPT2 forecasting generalist. *In total we use or train 14 baselines for forecasting.* **Datasets.** We evaluate on 7 benchmark datasets: weather [W], electricity [E], traffic [T], ETTm1 [m1], ETTm2 [m2], ETTh1 [h1], ETTh2 [h2]; and 5 zero shot datasets neuro2 [N2], neuro5 [N5] Peterson et al. (2022), and saugeen river flow [R], U.S. births [B], and sunspot [S] Godahewa et al. (2021). *In total we use 12 datasets for forecasting.* **Metrics.** Consistent with prior work, we report mean squared error MSE (lower is better \downarrow), mean absolute error MAE (\downarrow).

5 Results

Through experiments in imputation (§5.1), anomaly detection (§5.2), and forecasting (§5.3), our goal is to explore the efficacy of TOTEM on new general settings, as well as standard specialist benchmarks. To briefly refresh: specialist refers to training on a single domain (Tables 2D, 6, 10). Generalist refers to training on multiple domains (Tables 2B&C, 7, 11). Finally, in-domain refers to testing on the training domain, and zero-shot to testing on a separate domain from training, for a recap see Figure 1. We compare to two families of approaches: methods designed for multiple tasks (**multitask**) – TOTEM belongs in this category – and methods designed for a specific task (**singletask**), which may be adapted to other tasks. We present summary results in Figures 2A, 5, 6, for the full tables see the Appendix. For all experiments & models in the main paper, we run three seeds and report the mean; standard deviations in the Appendix. Since evaluation metrics differ across tasks, (\downarrow) will denote a metric where lower is better and (\uparrow) will denote a metric where higher is better. Given the varied metrics we calculate the average number of best results, or **AvgWins**, for each method and highlight the **best**, **second** best, and **third** best methods. In the following subsections we will discuss the baselines, datasets, and metrics for each task. We emphasize that no domain, sampling rate, or sensor dimension is shared between the training sets and zero-shot testing sets, see Table 3 for additional dataset details. For additional architecture and training details see §A.9 & §A.10.

5.1 Imputation

In imputation, models intake a masked time series $\mathbf{x}_m \in \mathbb{R}^{S \times T_{in}}$, and then reconstruct and impute $\mathbf{x} \in \mathbb{R}^{S \times T_{in}}$, see Figure 12. We experiment with four canonical masking percentages at 12.5%, 25%, 37.5%, 50%, and report MSE and MAE. **Specialist.** In Figure2A & Table 2D we compare TOTEM to baselines. All models are trained and evaluated on the same dataset (in-domain). TOTEM has the highest **AvgWins** with 52.1%, followed by GPT2 at 35.4%, and TiNet at 18.8%. TOTEM performance for m1 and h1 is lower; notably these datasets are the minute and hour resampling of the same raw data respectively. We investigate and discuss TOTEM’s success across different domains in Table 21. **Generalist.** In Figure2A & Table 2B&C we compare TOTEM to GPT2 (best performing models above), when both models are trained on the aggregate of W, E, m1, m2, h1, h2. We test them on the in-domain and zero-shot test sets. TOTEM outperforms GPT2 in-domain, 58.3% vs. 43.8%, and by a much larger margin in zero-shot, 80% vs. 20%. TOTEM’s performance across all experiments demonstrate that tokens are a performant representation for imputation. We visualize codebook examples in Figure 14, and imputation examples in Figure 15.

(Wu & Keogh, 2021) as Wu and Keogh identified flaws in the canonical anomaly detection benchmarks; TOTEM is SOTA or comparable across the 15 new benchmarks. We include all datasets to enable comparison to prior work, as well as promote the usage of new benchmarks.

Specialist. In Figure 5 & Table 6 we evaluate TOTEM against numerous specialist baselines. TOTEM has the highest **AvgWins** at 33.3% followed by a tie between GPT2, TiNet, ATrans, ETS, and LogTr at 13.3%.

Generalist. In Figure 5 & Table 7 we compare generalist-trained TOTEM and GPT2. On the in-domain test sets TOTEM outperforms 80% to 20%. In the zero-shot test sets TOTEM outperforms 73.3% to 26.7%. TOTEM’s **AvgWins** across the specialist and generalist settings demonstrate that tokens are a performant representation for anomaly detection. We visualize codebook examples in Figure 14.

5.3 Forecasting

In forecasting, models intake a time series $\mathbf{x} \in \mathbb{R}^{S \times T_{in}}$ and predict future readings $\mathbf{y} \in \mathbb{R}^{S \times T_{out}}$, where S is the number of sensors and T_{in}, T_{out} signify the durations of the preceding and succeeding time series, respectively. The pairs (\mathbf{x}, \mathbf{y}) are generated by striding the original time series data. All models have a lookback of $T_{in} = 96$, with prediction lengths $T_{out} = \{96, 192, 336, 720\}$. Numbers for other methods are from Liu et al. (2023). We run GPT2 with $T_{in} = 96$ as they originally report varying, dataset-specific, lookback lengths. We report MSE (\downarrow) and MAE (\downarrow). See Figure 6 for an overview.

Specialist. From Figure 6 & Table 10 we find that TOTEM achieves the highest **AvgWins** at 28.6% followed by iTrans at 26.8%. TOTEM has first finishes in five datasets while iTrans’ first finishes are concentrated in only electricity and traffic. **Generalist.** In Figure 6 & Table 11 we compare generalist TOTEM and GPT2. TOTEM outperforms GPT2 for both in-domain (67.9% vs. 33.9%) and zero-shot (90.0% vs. 12.5%). TOTEM’s **AvgWins** forecasting performance across the training and testing regimes demonstrates that tokens are a performant representation for forecasting. See example codebooks and forecasts in Figures 14 and 15.

6 Ablations

Discrete Tokens vs. Patches To evaluate if tokens enable TOTEM’s performance, we implement PatchTOTEM. PatchTOTEM has the identical architecture to TOTEM, except we replace the VQVAE with an MLP trained end-to-end with the downstream forecaster. We compare Totem vs. PatchTOTEM in the specialist in-domain, and generalist in-domain and zero-shot regimes, Figure 7 & Table 17. In all cases TOTEM outperforms PatchTOTEM - specialist: 67.9% vs. 39.3%, generalist in-domain: 78.6% vs. 23.2%, generalist zero-shot: 67.5% vs. 35.0%. TOTEM’s performance demonstrates that tokens, when compared to patches, lead to better performance.

Downstream Architecture & Discrete Tokens vs. Patches. In Figure 8 & Table 17 we explore the affect of discrete tokens versus patches for two separate forecasting

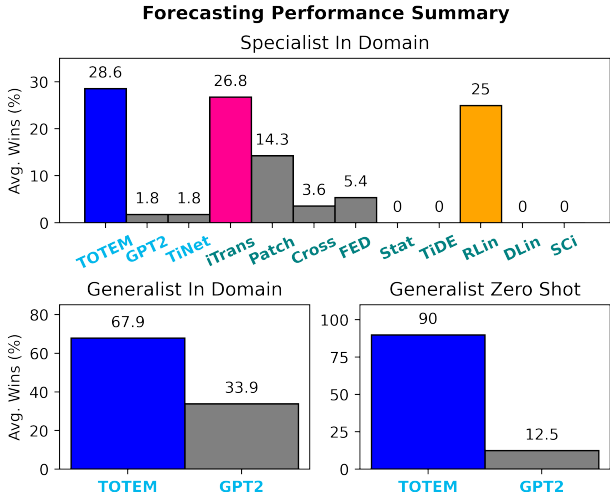


Figure 6: **Forecasting Summary.** In all categories TOTEM has SOTA **AvgWins**. In the specialist TOTEM has 28.6%; in generalist in domain TOTEM has 67.9%; in generalist zero shot TOTEM has 90.0%.

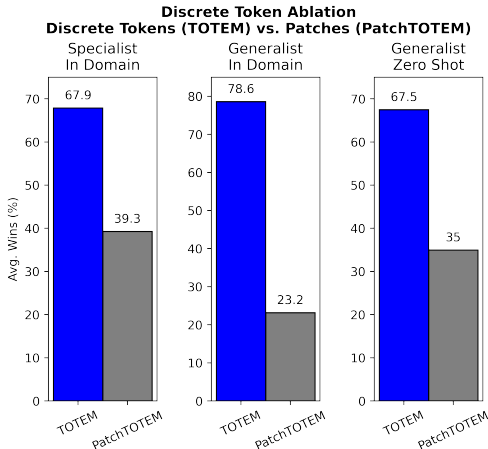


Figure 7: **Discrete Token Ablation.** In all categories the discrete token representation (TOTEM) has SOTA **AvgWins** over the patch representation (PatchTOTEM).

architectures the transformer encoder discussed above, §3.3 & Figure 4, and an MLP. The MLP has 3-layers with ReLUs, uses dropout with $p=0.1$ after the second layer, and concludes with a layernorm; the architecture is modeled after similar parsimonious forecasters in the literature like (Das et al., 2023a). The no-token MLP takes in uncompressed time series. The purpose of these ablations are not to compare the transformer to the MLP, but within each architecture to compare whether or not the discrete tokenized representation or the patch representation leads to better performance. We find that for both architectures the discrete token representation outperforms the patch representation; in the transformer 67.9% to 39.3% AvgWins and MLP 66.1% to 37.5% AvgWins .

Discrete Token Ablation While Varying Downstream Model Discrete Tokens (TOTEM) vs. Patches (PatchTOTEM)

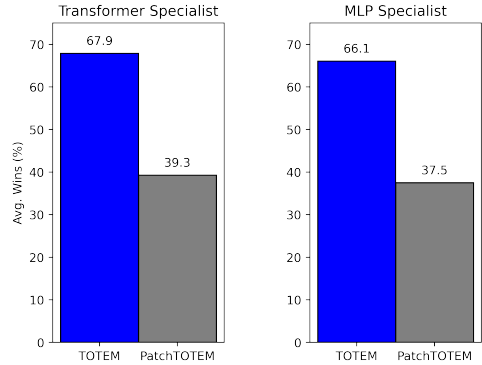


Figure 8: **Discrete Token vs. Patches with MLP.** For both the transformer (left) and MLP (right) the discrete token representation (TOTEM) outperforms the patch representation (PatchTOTEM).

Codebook Size. In Figure 9 left & Table 17 we explore the affect of the codebook size, K , on the VQVAE’s MSE and MAE reconstruction performance. As expected, we find that as K increases from 32 to 256 to 512 the reconstruction performance improves. However during downstream tasks, e.g. forecasting, it is beneficial to model the interactions between fewer codewords. Therefore we use $K = 256$ codewords. In Figure 9 middle we plot the average generalist codebook error over the downstream forecasting error demonstrating that most error does not come from a shared representation but the difficulty of the downstream task. This gives evidence that time series can have a single unified representation across multiple domains, akin to BPE in language modeling. In Figure 9 right, we plot the specialist codebook errors over the downstream forecasting errors to demonstrate that the finding of most error coming from the difficulty of the downstream task is not just a phenomenon found in the generalist.

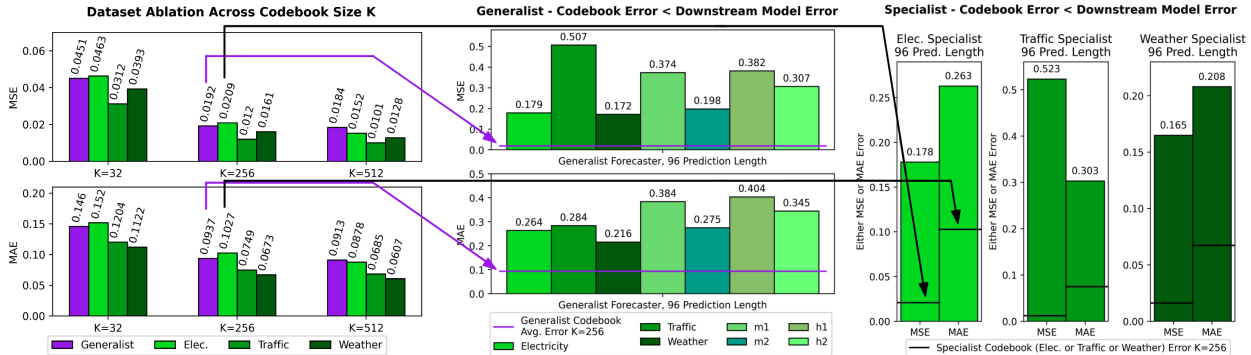


Figure 9: **Codebook Ablation.** Left, as the codebook size, K , increases the reconstruction performance of the VQVAE decreases. Middle, the generalist codebook error is smaller than the generalist forecasting error, demonstrating the promise of a single unified pre-trained representation for general time series. Right the specialist codebook error is smaller the the specialist codebook error.

7 Exploratory Studies in Generalist Modeling

Generalist Codebooks. To further explore the capabilities of a generalist codebook data representation we train models that utilize a general codebook but dataset-specific transformer forecasters, e.g. a TOTEM VQVAE trained on multiple domains with a forecaster trained only on electricity, Figure 10 & Table 20. We compare these mixed models to generalist and specialist models trained on the same domains. All models use the same

Generalist Codebooks Beat Specialist Codebooks

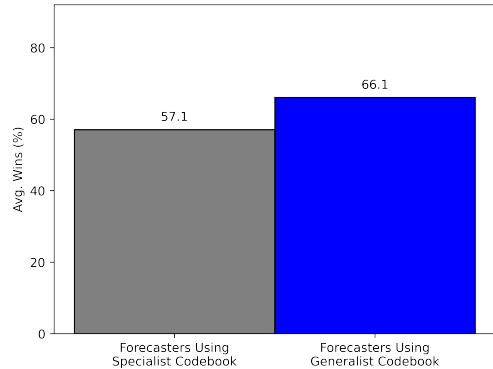


Figure 10: Generalist codebooks outperform specialist codebooks.

codebook hyperparameters (number of codewords $K = 256$, compression factor $F = 4$, code dimensionality $D = 64$) as well as the forecaster transformer architecture to ensure a fair comparison.

Since we are evaluating specialists, mixed-models, and a generalist on in-domain test data one might expect the TOTEM specialists to significantly outperform all models. Surprisingly this intuition is not correct. When comparing models trained using specialist codebooks to models trained using a single generalist codebook we find that generalist codebook models outperform specialists: 66.1% vs. 57.1%. Upon further inspection we find that the fully-generalist model (right Table 20) significantly outperforms the mixed-models (middle Table 20) in traffic (T) and electricity (E). This performance is puzzling until considering the training sizes.

The largest training set across domains belongs to traffic (T) at $10.2M$ training examples. In dataset T, the fully generalist models achieves 100% **AvgWins** . The second largest training set belongs to electricity (E) at $5.8M$ training examples, with 75% **AvgWins** for the fully-generalist model. Unfortunately there is a sharp drop off in training set sizes, with the rest of the data domains collectively comprising $1.6M$ training examples. These results evoke questions. For instance: does training on the smaller datasets act like form of regularization? Or: how does in-domain generalist performance scale with dataset size? We leave these exciting directions for future work. The generalist codebook’s performance across datasets highlights the potential of unified, discrete, token representations for in-domain evaluations.

Zero Shot Vignette: Training Size & Data Diversity.

Here we further explore generalist and specialist zero-shot testing capabilities, Figure 11 & Table 21. We take the two largest TOTEM specialist, traffic at $10.2M$ and electricity at $5.8M$ training examples, and test their zero-shot capabilities compared to the TOTEM generalist. We expect that the generalist will perform best as it was trained on the most data at $17.6M$ training examples as well as the most domains. We predict the generalist will be followed by TOTEM-traffic then TOTEM-electricity as they are both trained on only one domain but traffic has $4.4M$ more training examples than electricity. As expected the generalist outperforms both TOTEM-traffic and TOTEM-electricity with 85.0% **AvgWins** . However, curiously TOTEM-electricity outperforms TOTEM-traffic: 12.5% vs. 2.5% despite having $4.4M$ fewer training examples. Why is the smaller training set outperforming the larger training set? One possible explanation is that the electricity domain is more similar than the traffic domain to neuro, river, births, and sunspot. Another possible explanation comes from the raw time series dimensionality. Despite having fewer training examples, electricity has a higher number of raw time steps⁴ compared to traffic: 26304 vs. 17544. However, traffic has a larger number of sensors: 862 vs. 321. This limited analysis suggests that a higher number of raw time steps is more valuable than more sensor readings. Untangling these possibilities and beginning to answer the questions: what is a unit of data in time series? And how does this unit scale as the time steps, sensors, and examples scale? are valuable future directions. The zero shot vignette has demonstrated the power of the token-enabled generalist over the traffic and electricity specialists, and has opened up exciting training size and data diversity questions.

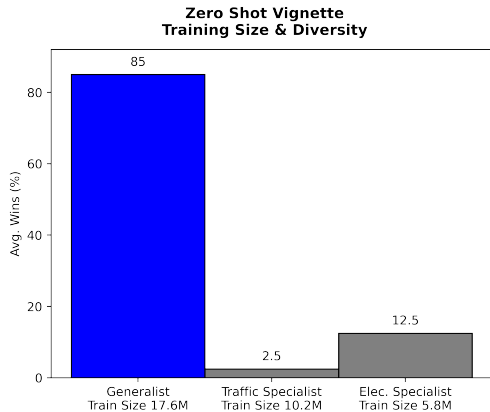


Figure 11: **Zero Shot Vignette.** The generalist has the highest zero shot performance at 85.0% **AvgWins** , when compared to the two largest specialists: Traffic and Elec.

8 Conclusion

We present TOTEM: a simple, performant tokenizer that works across domains thereby enabling generalist modeling across tasks. TOTEM demonstrates strong in-domain and zero-shot capabilities that match or outperform existing state-of-the-art approaches. Moving forward, an interesting limitation is that TOTEM does not support variable token lengths. Dynamic token lengths could potentially enhance unified data representations and further improve task performance. Other interesting directions include further investigating the relationship between generalist data representations, token length, data size, and domain diversity.

⁴Raw time steps for all data. The train:val:test ratio is 7:1:2.

9 Broader Impact Statement

There are no immediate ethical concerns that arise from our work. However, as with all data driven methods, certain societal consequences are important to be discussed, in this case surrounding time series modeling. A few are reported below:

Privacy Concerns. Time series data, especially when sourced from personal devices or applications, can contain sensitive information about individuals, e.g. for health domains. In this work, no time series were sourced from personal devices.

Misuse. Time series forecast models can be misused. For instance, if a model forecasts stock prices or market movements, it could be exploited for insider trading or other illegal financial activities. In this work, we are focused on domains pertinent to scientific disciplines.

Economic Impacts. Automated forecasts and decisions based on time series models can significantly impact industries and labor markets both positively and negatively. For instance, if a model can accurately predict weather patterns, it might affect farmers and their crop decisions, or if it can forecast energy consumption, it could impact the energy sector.

References

- Oliver D Anderson. Time-series. 2nd edn., 1976.
- Abdul Fatir Ansari, Lorenzo Stella, Caner Turkmen, Xiyuan Zhang, Pedro Mercado, Huibin Shen, Oleksandr Shchur, Syama Sundar Rangapuram, Sebastian Pineda Arango, Shubham Kapoor, et al. Chronos: Learning the language of time series. *arXiv preprint arXiv:2403.07815*, 2024.
- Alexei Baevski, Yuhao Zhou, Abdelrahman Mohamed, and Michael Auli. wav2vec 2.0: A framework for self-supervised learning of speech representations. *Advances in neural information processing systems*, 33: 12449–12460, 2020.
- Shaojie Bai, J Zico Kolter, and Vladlen Koltun. An empirical evaluation of generic convolutional and recurrent networks for sequence modeling. *arXiv preprint arXiv:1803.01271*, 2018.
- George Barnum, Sabera Talukder, and Yisong Yue. On the benefits of early fusion in multimodal representation learning. *arXiv preprint arXiv:2011.07191*, 2020.
- Wei Cao, Dong Wang, Jian Li, Hao Zhou, Lei Li, and Yitan Li. Brits: Bidirectional recurrent imputation for time series. *Advances in neural information processing systems*, 31, 2018.
- Cristian Challu, Kin G Olivares, Boris N Oreshkin, Federico Garza Ramirez, Max Mergenthaler Canseco, and Artur Dubrawski. Nhits: Neural hierarchical interpolation for time series forecasting. In *Proceedings of the AAAI Conference on Artificial Intelligence*, volume 37, pp. 6989–6997, 2023.
- Cristian I Challu, Peihong Jiang, Ying Nian Wu, and Laurent Callot. Deep generative model with hierarchical latent factors for time series anomaly detection. In *International Conference on Artificial Intelligence and Statistics*, pp. 1643–1654. PMLR, 2022.
- Geeling Chau, Yujin An, Ahamed Raffey Iqbal, Soon-Jo Chung, Yisong Yue, and Sabera Talukder. Generalizability under sensor failure: Tokenization+ transformers enable more robust latent spaces. *arXiv preprint arXiv:2402.18546*, 2024.
- Si-An Chen, Chun-Liang Li, Nate Yoder, Sercan O Arik, and Tomas Pfister. Tsmixer: An all-mlp architecture for time series forecasting. *arXiv preprint arXiv:2303.06053*, 2023.
- Tae-Min Choi, Ji-Su Kang, and Jong-Hwan Kim. Rdis: Random drop imputation with self-training for incomplete time series data. *IEEE Access*, 2023.
- Abhimanyu Das, Weihao Kong, Andrew Leach, Rajat Sen, and Rose Yu. Long-term forecasting with tide: Time-series dense encoder. *arXiv preprint arXiv:2304.08424*, 2023a.

- Abhimanyu Das, Weihao Kong, Rajat Sen, and Yichen Zhou. A decoder-only foundation model for time-series forecasting. *arXiv preprint arXiv:2310.10688*, 2023b.
- Alexey Dosovitskiy, Lucas Beyer, Alexander Kolesnikov, Dirk Weissenborn, Xiaohua Zhai, Thomas Unterthiner, Mostafa Dehghani, Matthias Minderer, Georg Heigold, Sylvain Gelly, et al. An image is worth 16x16 words: Transformers for image recognition at scale. *arXiv preprint arXiv:2010.11929*, 2020.
- Vijay Ekambaram, Arindam Jati, Nam Nguyen, Phanwadee Sinthong, and Jayant Kalagnanam. Tsmixer: Lightweight mlp-mixer model for multivariate time series forecasting. In *Proceedings of the 29th ACM SIGKDD Conference on Knowledge Discovery and Data Mining*, pp. 459–469, 2023.
- Patrick Esser, Robin Rombach, and Bjorn Ommer. Taming transformers for high-resolution image synthesis. In *Proceedings of the IEEE/CVF conference on computer vision and pattern recognition*, pp. 12873–12883, 2021.
- Jean-Yves Franceschi, Aymeric Dieuleveut, and Martin Jaggi. Unsupervised scalable representation learning for multivariate time series. *Advances in neural information processing systems*, 32, 2019.
- Philip Gage. A new algorithm for data compression. *C Users Journal*, 12(2):23–38, 1994.
- Rakshitha Godahewa, Christoph Bergmeir, Geoffrey I. Webb, Rob J. Hyndman, and Pablo Montero-Manso. Monash time series forecasting archive. In *Neural Information Processing Systems Track on Datasets and Benchmarks*, 2021.
- Mononito Goswami, Konrad Szafer, Arjun Choudhry, Yifu Cai, Shuo Li, and Artur Dubrawski. Moment: A family of open time-series foundation models. *arXiv preprint arXiv:2402.03885*, 2024.
- Yangdong He and Jiabao Zhao. Temporal convolutional networks for anomaly detection in time series. In *Journal of Physics: Conference Series*, volume 1213, pp. 042050. IOP Publishing, 2019.
- Sepp Hochreiter and Jürgen Schmidhuber. Long short-term memory. *Neural computation*, 9(8):1735–1780, 1997.
- Charles C Holt. Forecasting trends and seasonals by exponentially weighted moving averages. *ONR Memorandum*, 52(52):5–10, 1957.
- Rob J Hyndman and George Athanasopoulos. *Forecasting: principles and practice*. OTexts, 2018.
- Taesung Kim, Jinhee Kim, Yunwon Tae, Cheonbok Park, Jang-Ho Choi, and Jaegul Choo. Reversible instance normalization for accurate time-series forecasting against distribution shift. In *International Conference on Learning Representations*, 2021.
- Nikita Kitaev, Łukasz Kaiser, and Anselm Levskaya. Reformer: The efficient transformer. *arXiv preprint arXiv:2001.04451*, 2020.
- Shiyang Li, Xiaoyong Jin, Yao Xuan, Xiyou Zhou, Wenhui Chen, Yu-Xiang Wang, and Xifeng Yan. Enhancing the locality and breaking the memory bottleneck of transformer on time series forecasting. *Advances in neural information processing systems*, 32, 2019.
- Zhe Li, Shiyi Qi, Yiduo Li, and Zenglin Xu. Revisiting long-term time series forecasting: An investigation on linear mapping. *arXiv preprint arXiv:2305.10721*, 2023.
- Jessica Lin, Eamonn Keogh, Li Wei, and Stefano Lonardi. Experiencing sax: a novel symbolic representation of time series. *Data Mining and knowledge discovery*, 15:107–144, 2007.
- Minhao Liu, Ailing Zeng, Muxi Chen, Zhijian Xu, Qiuxia Lai, Lingna Ma, and Qiang Xu. Scinet: Time series modeling and forecasting with sample convolution and interaction. *Advances in Neural Information Processing Systems*, 35:5816–5828, 2022a.

- Shizhan Liu, Hang Yu, Cong Liao, Jianguo Li, Weiyao Lin, Alex X Liu, and Schahram Dustdar. Pyraformer: Low-complexity pyramidal attention for long-range time series modeling and forecasting. In *International conference on learning representations*, 2021.
- Yong Liu, Haixu Wu, Jianmin Wang, and Mingsheng Long. Non-stationary transformers: Exploring the stationarity in time series forecasting. *Advances in Neural Information Processing Systems*, 35:9881–9893, 2022b.
- Yong Liu, Tengge Hu, Haoran Zhang, Haixu Wu, Shiyu Wang, Lintao Ma, and Mingsheng Long. itransformer: Inverted transformers are effective for time series forecasting. *arXiv preprint arXiv:2310.06625*, 2023.
- Yonghong Luo, Xiangrui Cai, Ying Zhang, Jun Xu, et al. Multivariate time series imputation with generative adversarial networks. *Advances in neural information processing systems*, 31, 2018.
- Yonghong Luo, Ying Zhang, Xiangrui Cai, and Xiaojie Yuan. E2gan: End-to-end generative adversarial network for multivariate time series imputation. In *Proceedings of the 28th international joint conference on artificial intelligence*, pp. 3094–3100. AAAI Press Palo Alto, CA, USA, 2019.
- Ahmad Wisnu Mulyadi, Eunji Jun, and Heung-Il Suk. Uncertainty-aware variational-recurrent imputation network for clinical time series. *IEEE Transactions on Cybernetics*, 52(9):9684–9694, 2021.
- Yuqi Nie, Nam H Nguyen, Phanwadee Sinthong, and Jayant Kalagnanam. A time series is worth 64 words: Long-term forecasting with transformers. *arXiv preprint arXiv:2211.14730*, 2022.
- Aaron van den Oord, Sander Dieleman, Heiga Zen, Karen Simonyan, Oriol Vinyals, Alex Graves, Nal Kalchbrenner, Andrew Senior, and Koray Kavukcuoglu. Wavenet: A generative model for raw audio. *arXiv preprint arXiv:1609.03499*, 2016.
- Boris N Oreshkin, Dmitri Carpov, Nicolas Chapados, and Yoshua Bengio. N-beats: Neural basis expansion analysis for interpretable time series forecasting. *arXiv preprint arXiv:1905.10437*, 2019.
- Steven M Peterson, Satpreet H Singh, Benjamin Dichter, Michael Scheid, Rajesh PN Rao, and Bingni W Brunton. Ajile12: Long-term naturalistic human intracranial neural recordings and pose. *Scientific data*, 9(1):184, 2022.
- S Rabanser, T Januschowski, V Flunkert, D Salinas, and J Gasthaus. The effectiveness of discretization in forecasting: An empirical study on neural time series models. arxiv 2020. *arXiv preprint arXiv:2005.10111*, 2020.
- Alec Radford, Karthik Narasimhan, Tim Salimans, Ilya Sutskever, et al. Improving language understanding by generative pre-training. 2018.
- Robin Rombach, Andreas Blattmann, Dominik Lorenz, Patrick Esser, and Björn Ommer. High-resolution image synthesis with latent diffusion models. In *Proceedings of the IEEE/CVF conference on computer vision and pattern recognition*, pp. 10684–10695, 2022.
- David Salinas, Valentin Flunkert, Jan Gasthaus, and Tim Januschowski. Deepar: Probabilistic forecasting with autoregressive recurrent networks. *International Journal of Forecasting*, 36(3):1181–1191, 2020.
- Lifeng Shen, Zhuocong Li, and James Kwok. Timeseries anomaly detection using temporal hierarchical one-class network. *Advances in Neural Information Processing Systems*, 33:13016–13026, 2020.
- Ikaro Silva, George Moody, Daniel J Scott, Leo A Celi, and Roger G Mark. Predicting in-hospital mortality of icu patients: The physionet/computing in cardiology challenge 2012. In *2012 computing in cardiology*, pp. 245–248. IEEE, 2012.
- Sabera Talukder, Jennifer J Sun, Matthew Leonard, Bingni W Brunton, and Yisong Yue. Deep neural imputation: A framework for recovering incomplete brain recordings. *arXiv preprint arXiv:2206.08094*, 2022.

- Yusuke Tashiro, Jiaming Song, Yang Song, and Stefano Ermon. CSDI: Conditional score-based diffusion models for probabilistic time series imputation. *Advances in Neural Information Processing Systems*, 34: 24804–24816, 2021.
- Sean J Taylor and Benjamin Letham. Forecasting at scale. *The American Statistician*, 72(1):37–45, 2018.
- Sana Tonekaboni, Danny Eytan, and Anna Goldenberg. Unsupervised representation learning for time series with temporal neighborhood coding. *arXiv preprint arXiv:2106.00750*, 2021.
- Aaron Van Den Oord, Oriol Vinyals, et al. Neural discrete representation learning. *Advances in neural information processing systems*, 30, 2017.
- Ashish Vaswani, Noam Shazeer, Niki Parmar, Jakob Uszkoreit, Llion Jones, Aidan N Gomez, Łukasz Kaiser, and Illia Polosukhin. Attention is all you need. *Advances in neural information processing systems*, 30, 2017.
- Peter R Winters. Forecasting sales by exponentially weighted moving averages. *Management science*, 6(3): 324–342, 1960.
- Gerald Woo, Chenghao Liu, Doyen Sahoo, Akshat Kumar, and Steven Hoi. Etsformer: Exponential smoothing transformers for time-series forecasting. *arXiv preprint arXiv:2202.01381*, 2022.
- Haixu Wu, Jiehui Xu, Jianmin Wang, and Mingsheng Long. Autoformer: Decomposition transformers with auto-correlation for long-term series forecasting. *Advances in Neural Information Processing Systems*, 34: 22419–22430, 2021.
- Haixu Wu, Tengge Hu, Yong Liu, Hang Zhou, Jianmin Wang, and Mingsheng Long. Timesnet: Temporal 2d-variation modeling for general time series analysis. *arXiv preprint arXiv:2210.02186*, 2022a.
- Haixu Wu, Jialong Wu, Jiehui Xu, Jianmin Wang, and Mingsheng Long. Flowformer: Linearizing transformers with conservation flows. *arXiv preprint arXiv:2202.06258*, 2022b.
- Renjie Wu and Eamonn J Keogh. Current time series anomaly detection benchmarks are flawed and are creating the illusion of progress. *IEEE transactions on knowledge and data engineering*, 35(3):2421–2429, 2021.
- Jiehui Xu, Haixu Wu, Jianmin Wang, and Mingsheng Long. Anomaly transformer: Time series anomaly detection with association discrepancy. *arXiv preprint arXiv:2110.02642*, 2021.
- Ling Yang and Shenda Hong. Unsupervised time-series representation learning with iterative bilinear temporal-spectral fusion. In *International Conference on Machine Learning*, pp. 25038–25054. PMLR, 2022.
- Zhihan Yue, Yujing Wang, Juanyong Duan, Tianmeng Yang, Congrui Huang, Yunhai Tong, and Bixiong Xu. Ts2vec: Towards universal representation of time series. In *Proceedings of the AAAI Conference on Artificial Intelligence*, volume 36, pp. 8980–8987, 2022.
- Ailing Zeng, Muxi Chen, Lei Zhang, and Qiang Xu. Are transformers effective for time series forecasting? In *Proceedings of the AAAI conference on artificial intelligence*, volume 37, pp. 11121–11128, 2023.
- Tianping Zhang, Yizhuo Zhang, Wei Cao, Jiang Bian, Xiaohan Yi, Shun Zheng, and Jian Li. Less is more: Fast multivariate time series forecasting with light sampling-oriented mlp structures. *arXiv preprint arXiv:2207.01186*, 2022.
- Yunhao Zhang and Junchi Yan. Crossformer: Transformer utilizing cross-dimension dependency for multivariate time series forecasting. In *The Eleventh International Conference on Learning Representations*, 2022.
- Haoyi Zhou, Shanghang Zhang, Jieqi Peng, Shuai Zhang, Jianxin Li, Hui Xiong, and Wancai Zhang. Informer: Beyond efficient transformer for long sequence time-series forecasting. In *Proceedings of the AAAI conference on artificial intelligence*, volume 35, pp. 11106–11115, 2021.

Tian Zhou, Ziqing Ma, Qingsong Wen, Xue Wang, Liang Sun, and Rong Jin. Fedformer: Frequency enhanced decomposed transformer for long-term series forecasting. In *International Conference on Machine Learning*, pp. 27268–27286. PMLR, 2022.

Tian Zhou, Peisong Niu, Xue Wang, Liang Sun, and Rong Jin. One fits all: Power general time series analysis by pretrained lm. *arXiv preprint arXiv:2302.11939*, 2023.

A Appendix

A.1 Dataset.

Dataset	Sampling Rate	Number Sensors
Imputation & Forecasting Training Sets		
Weather	Every 10 min	21
Traffic	Every hour	862
Electricity	Every hour	321
Etth1, ETTh2	Every hour	7
Ettm1, ETTm2	Every 15 min	7
Anomaly Detection Training Sets		
SMD (Sever Machine)	Every min	38
MSL (Mars Rover)	Every min	55
SMAP (Soil Moisture)	Every min	25
SWAT (Water Treatment)	Every sec	51
PSM (Pooled Server)	Every min	25
Zero Shot Testing Sets for Imputation, Forecasting & Anomaly Detection		
Neuro2	Every 0.002 sec	72
Neuro5	Every 0.002 sec	106
Sageen River Flow	Every day	1
US Birth Rate	Every day	1
Sunspot	Every day	1

Table 3: Dataset Information Table. Notably no sampling rate or sensor number is shared between the training sets and testing sets for any task.

A.2 Imputation.

Imputer

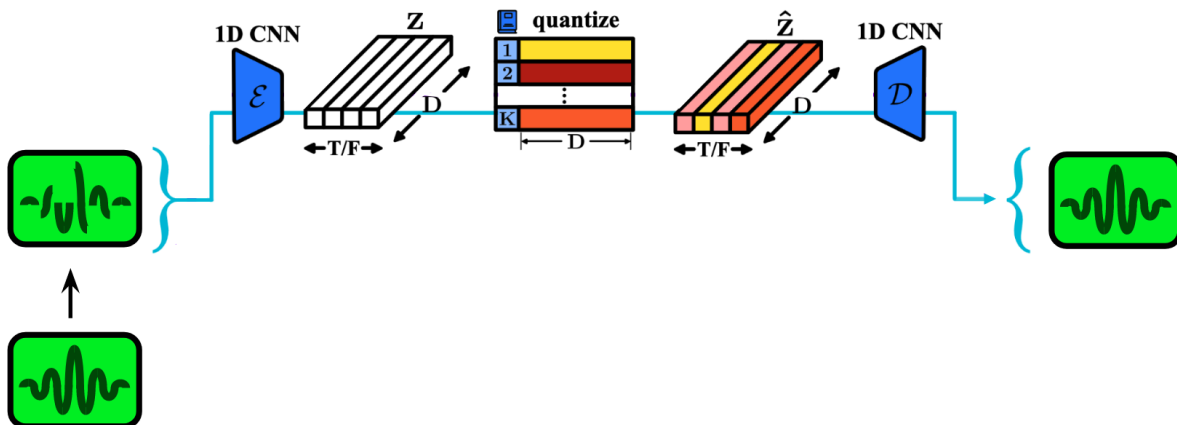


Figure 12: **Imputation Visualization.** The VQVAE architecture does not change for the imputation task. The data passed in has a mask applied to it so that the VQVAE solves the task of reconstruction and imputation simultaneously.

Table 4: **Means & Stds. for the Imputation Task.** A. is the TOTEM specialist, B. is the TOTEM generalist, C. is the GPT2 generalist which we setup to run in a generalist manner.

A. TOTEM - Specialist Imputation (\downarrow)			B. TOTEM - Generalist Imputation (\downarrow)			C. GPT2 - Generalist Imputation (\downarrow)			
Metric	MSE	MAE	Metric	MSE	MAE	Metric	MSE	MAE	
W	12.5%	0.028 \pm 0.0000	0.046 \pm 0.0006	12.5%	0.029 \pm 0.0012	0.060 \pm 0.0047	12.5%	0.029 \pm 0.0000	0.045 \pm 0.0006
	25%	0.029 \pm 0.0000	0.047 \pm 0.0010	25%	0.030 \pm 0.0006	0.060 \pm 0.0047	25%	0.033 \pm 0.0006	0.048 \pm 0.0006
	37.5%	0.067 \pm 0.0006	0.048 \pm 0.0015	37.5%	0.032 \pm 0.0006	0.062 \pm 0.0030	37.5%	0.037 \pm 0.0006	0.054 \pm 0.0012
E	12.5%	0.054 \pm 0.0006	0.154 \pm 0.0015	12.5%	0.065 \pm 0.0020	0.171 \pm 0.0032	12.5%	0.008 \pm 0.0020	0.186 \pm 0.0035
	25%	0.059 \pm 0.0006	0.160 \pm 0.0010	25%	0.071 \pm 0.0015	0.179 \pm 0.0031	25%	0.091 \pm 0.0020	0.197 \pm 0.0025
	37.5%	0.067 \pm 0.0006	0.169 \pm 0.0012	37.5%	0.080 \pm 0.0025	0.189 \pm 0.0032	37.5%	0.108 \pm 0.0021	0.213 \pm 0.0026
m1	12.5%	0.049 \pm 0.0000	0.125 \pm 0.0006	12.5%	0.041 \pm 0.0006	0.132 \pm 0.0015	12.5%	0.052 \pm 0.0012	0.141 \pm 0.0016
	25%	0.052 \pm 0.0006	0.128 \pm 0.0006	25%	0.044 \pm 0.0000	0.135 \pm 0.0010	25%	0.065 \pm 0.0021	0.154 \pm 0.0021
	37.5%	0.055 \pm 0.0000	0.132 \pm 0.0006	37.5%	0.048 \pm 0.0006	0.139 \pm 0.0040	37.5%	0.085 \pm 0.0038	0.171 \pm 0.0026
m2	12.5%	0.016 \pm 0.0006	0.078 \pm 0.0010	12.5%	0.040 \pm 0.0020	0.125 \pm 0.0067	12.5%	0.029 \pm 0.0000	0.095 \pm 0.0006
	25%	0.017 \pm 0.0006	0.081 \pm 0.0006	25%	0.041 \pm 0.0015	0.126 \pm 0.0058	25%	0.033 \pm 0.0006	0.101 \pm 0.0006
	37.5%	0.018 \pm 0.0000	0.084 \pm 0.0006	37.5%	0.043 \pm 0.0015	0.129 \pm 0.0049	37.5%	0.038 \pm 0.0006	0.110 \pm 0.0012
h1	12.5%	0.119 \pm 0.0010	0.212 \pm 0.0006	12.5%	0.100 \pm 0.0049	0.201 \pm 0.0049	12.5%	0.113 \pm 0.0012	0.217 \pm 0.0021
	25%	0.127 \pm 0.0015	0.220 \pm 0.0006	25%	0.108 \pm 0.0049	0.209 \pm 0.0038	25%	0.131 \pm 0.0010	0.231 \pm 0.0015
	37.5%	0.138 \pm 0.0012	0.230 \pm 0.0006	37.5%	0.122 \pm 0.0064	0.220 \pm 0.0044	37.5%	0.153 \pm 0.0012	0.247 \pm 0.0017
h2	12.5%	0.040 \pm 0.0006	0.129 \pm 0.0017	12.5%	0.144 \pm 0.0078	0.237 \pm 0.0049	12.5%	0.182 \pm 0.0006	0.266 \pm 0.0012
	25%	0.041 \pm 0.0010	0.131 \pm 0.0012	25%	0.076 \pm 0.0006	0.177 \pm 0.0036	25%	0.071 \pm 0.0006	0.160 \pm 0.0015
	37.5%	0.043 \pm 0.0006	0.136 \pm 0.0006	37.5%	0.093 \pm 0.0222	0.195 \pm 0.0200	37.5%	0.077 \pm 0.0010	0.167 \pm 0.0015
N2	12.5%	0.020 \pm 0.0000	0.088 \pm 0.0000	12.5%	0.089 \pm 0.0010	0.192 \pm 0.0035	12.5%	0.086 \pm 0.0032	0.179 \pm 0.0038
	25%	0.017 \pm 0.0006	0.081 \pm 0.0006	25%	0.033 \pm 0.0010	0.127 \pm 0.0035	25%	0.064 \pm 0.0017	0.164 \pm 0.0015
	37.5%	0.018 \pm 0.0000	0.084 \pm 0.0006	37.5%	0.041 \pm 0.0006	0.139 \pm 0.0025	37.5%	0.090 \pm 0.0036	0.191 \pm 0.0032
N5	12.5%	0.119 \pm 0.0010	0.212 \pm 0.0006	12.5%	0.017 \pm 0.0010	0.085 \pm 0.0030	12.5%	0.021 \pm 0.0006	0.095 \pm 0.0012
	25%	0.127 \pm 0.0015	0.220 \pm 0.0006	25%	0.019 \pm 0.0010	0.090 \pm 0.0030	25%	0.028 \pm 0.0006	0.107 \pm 0.0010
	37.5%	0.138 \pm 0.0012	0.230 \pm 0.0006	37.5%	0.022 \pm 0.0006	0.098 \pm 0.0025	37.5%	0.039 \pm 0.0015	0.123 \pm 0.0015
R	12.5%	0.040 \pm 0.0006	0.129 \pm 0.0017	12.5%	0.071 \pm 0.0070	0.109 \pm 0.0040	12.5%	0.093 \pm 0.0010	0.119 \pm 0.0015
	25%	0.041 \pm 0.0010	0.131 \pm 0.0012	25%	0.087 \pm 0.0064	0.117 \pm 0.0031	25%	0.125 \pm 0.0006	0.134 \pm 0.0026
	37.5%	0.043 \pm 0.0006	0.136 \pm 0.0006	37.5%	0.112 \pm 0.0050	0.129 \pm 0.0035	37.5%	0.167 \pm 0.0021	0.154 \pm 0.0042
B	12.5%	0.047 \pm 0.0006	0.142 \pm 0.0012	12.5%	0.148 \pm 0.0032	0.147 \pm 0.0023	12.5%	0.220 \pm 0.0045	0.182 \pm 0.0057
	25%	0.048 \pm 0.0006	0.144 \pm 0.0012	25%	0.632 \pm 0.0087	0.642 \pm 0.0068	25%	0.392 \pm 0.0064	0.496 \pm 0.0023
	37.5%	0.049 \pm 0.0006	0.145 \pm 0.0012	37.5%	0.693 \pm 0.0070	0.665 \pm 0.0047	37.5%	0.444 \pm 0.0071	0.523 \pm 0.0029
S	12.5%	0.057 \pm 0.0012	0.160 \pm 0.0023	12.5%	0.632 \pm 0.0087	0.642 \pm 0.0068	12.5%	0.498 \pm 0.0080	0.553 \pm 0.0023
	25%	0.061 \pm 0.0006	0.168 \pm 0.0021	25%	0.761 \pm 0.0055	0.692 \pm 0.0023	25%	0.591 \pm 0.0700	0.599 \pm 0.0275
	37.5%	0.069 \pm 0.0006	0.178 \pm 0.0021	37.5%	0.827 \pm 0.0044	0.718 \pm 0.0000	37.5%	0.591 \pm 0.0700	0.599 \pm 0.0275
s	12.5%	0.057 \pm 0.0012	0.160 \pm 0.0023	12.5%	0.057 \pm 0.0012	0.160 \pm 0.0023	12.5%	0.070 \pm 0.0012	0.173 \pm 0.0017
	25%	0.061 \pm 0.0006	0.168 \pm 0.0021	25%	0.061 \pm 0.0006	0.168 \pm 0.0021	25%	0.084 \pm 0.0010	0.189 \pm 0.0015
	37.5%	0.069 \pm 0.0006	0.178 \pm 0.0021	37.5%	0.069 \pm 0.0006	0.178 \pm 0.0021	37.5%	0.103 \pm 0.0010	0.209 \pm 0.0021
Zero-Shot	12.5%	0.020 \pm 0.0000	0.088 \pm 0.0000	12.5%	0.029 \pm 0.0015	0.120 \pm 0.0045	12.5%	0.047 \pm 0.0006	0.145 \pm 0.0015
	25%	0.017 \pm 0.0006	0.081 \pm 0.0006	25%	0.033 \pm 0.0010	0.127 \pm 0.0035	25%	0.064 \pm 0.0017	0.164 \pm 0.0015
	37.5%	0.018 \pm 0.0000	0.084 \pm 0.0006	37.5%	0.041 \pm 0.0006	0.139 \pm 0.0025	37.5%	0.090 \pm 0.0036	0.191 \pm 0.0032
Zero-Shot	12.5%	0.020 \pm 0.0000	0.088 \pm 0.0000	12.5%	0.017 \pm 0.0010	0.085 \pm 0.0030	12.5%	0.021 \pm 0.0006	0.095 \pm 0.0012
	25%	0.017 \pm 0.0006	0.081 \pm 0.0006	25%	0.019 \pm 0.0010	0.090 \pm 0.0030	25%	0.028 \pm 0.0006	0.107 \pm 0.0010
	37.5%	0.018 \pm 0.0000	0.084 \pm 0.0006	37.5%	0.022 \pm 0.0006	0.098 \pm 0.0025	37.5%	0.039 \pm 0.0015	0.123 \pm 0.0015

Table 5: **Imputation on PhysioNet 2012 Dataset.** We report MAE where lower is better. TOTEM has the best performance in all three scenarios of percent missing.

Method	10% Missing	50% Missing	90% Missing
V-Rin	0.271	0.365	0.606
BRITS	0.284	0.368	0.517
RDIS	0.319	0.419	0.613
Unconditional	0.326	0.417	0.625
CSDI	0.217	0.301	0.481
TOTEM (Ours)	0.126	0.134	0.143

A.3 Anomaly Detection.

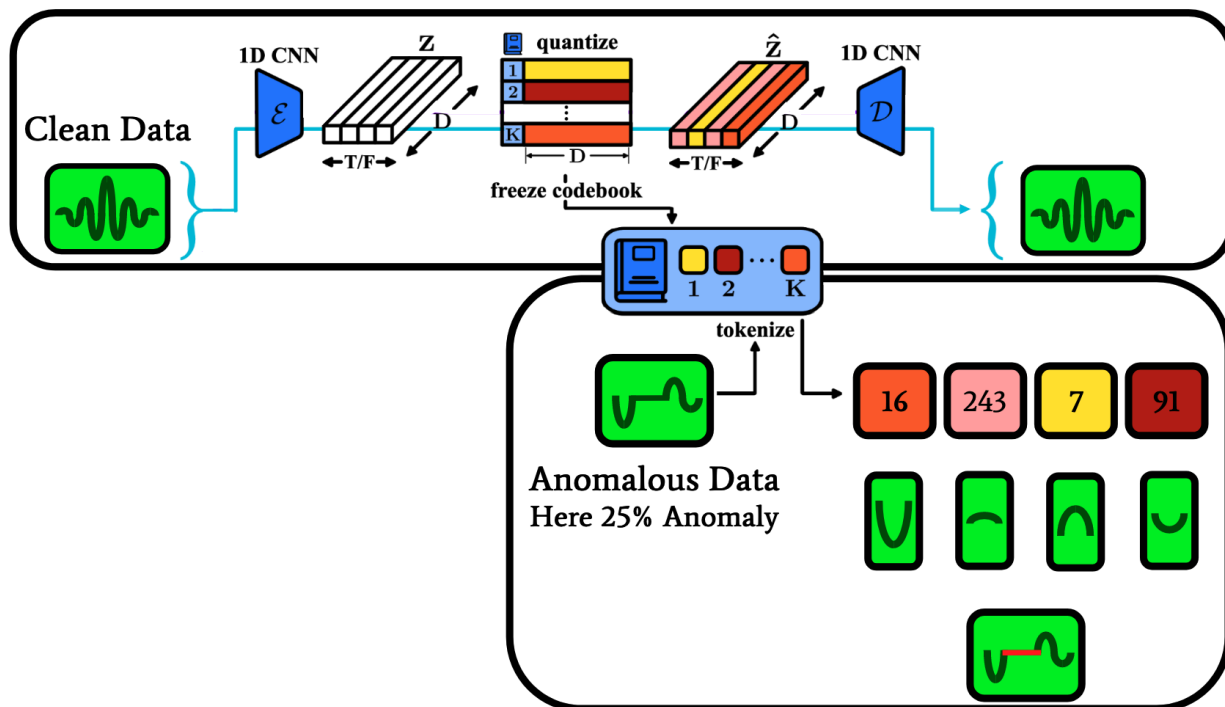
Anomaly Detector

Figure 13: **Anomaly Detection Visualization.** The VQVAE architecture does not change for the anomaly detection task. The training data passed in must be clean such that the VQVAE can learn clean representations. At test time, when anomaly data is passed in with anomaly A% (in this case 25%), the worst A% reconstructed is set to the anomaly.

Table 6: **Specialist Anomaly Detection** (\uparrow). TOTEM has the highest AvgWins at **33.3%** followed by a five-way tie between GPT2, TiNet, ATran, ETS, and LogTr at **13.3%**. Some prior methods use the test set as a validation set for early stopping of the learning algorithm, which can inflate performance. We do not adopt this practice and train TOTEM for a set number of iterations.

Model	TOTEM	GPT2	TiNet	ATran	Patch	ETS	FED	Stat	Auto	Pyra	Inf	Re	LogTr	Trans	LiTS	DLin	
F1	SMD	79.62	86.89	84.61	85.49	84.62	83.13	84.62	85.11	83.04	81.65	75.32	76.21	79.56	82.53	77.10	
	MSL	82.58	82.45	81.84	83.31	78.70	78.57	77.50	79.05	84.86	84.06	84.40	79.57	78.68	78.95	84.88	
	SMAP	94.02	72.88	69.39	71.18	68.82	69.50	70.76	71.09	71.12	71.09	69.92	70.40	69.97	69.70	69.21	69.26
	SWAT	94.27	94.23	93.02	83.10	85.72	84.91	93.19	79.88	92.74	91.78	81.43	82.80	80.52	80.37	93.33	87.52
	PSM	95.87	97.13	97.34	79.40	96.08	91.76	97.23	97.29	93.29	82.08	77.10	73.61	76.74	76.07	97.15	93.55
R	SMD	76.06	84.98	81.54	82.23	82.14	79.23	82.39	81.21	82.35	80.61	77.23	69.24	70.13	76.13	78.42	71.52
	MSL	82.85	82.91	75.36	87.37	70.96	84.93	80.07	89.14	80.92	85.93	86.48	83.31	87.37	87.37	79.78	85.42
	SMAP	94.04	60.95	56.40	58.11	55.46	55.75	58.10	59.02	58.62	57.71	57.13	57.44	57.59	57.12	55.27	55.41
	SWAT	95.91	96.34	95.40	97.32	80.94	80.36	96.42	96.75	95.81	96.00	96.75	96.53	97.32	96.53	94.72	95.30
	PSM	94.21	95.68	96.20	94.72	93.47	85.28	97.16	96.76	88.15	96.02	96.33	95.38	98.00	96.56	95.97	89.20
P	SMD	83.54	88.89	87.91	88.91	87.26	87.44	87.95	88.33	88.06	85.61	86.60	82.58	83.46	83.58	87.10	83.62
	MSL	82.32	82.00	89.54	79.61	88.34	85.13	77.14	68.55	77.27	83.81	81.77	85.51	73.05	71.57	82.40	84.34
	SMAP	94.00	90.60	90.14	91.85	90.64	92.25	90.47	89.37	90.40	92.54	90.11	90.91	89.15	89.37	92.58	92.32
	SWAT	92.68	92.20	90.75	72.51	91.10	90.02	90.17	68.03	89.85	87.92	70.29	72.50	68.67	68.84	91.98	80.91
	PSM	97.58	98.62	98.51	68.35	98.84	99.31	97.31	97.82	99.08	71.67	64.27	59.93	63.06	62.75	98.37	98.28
AvgWins	33.3%	13.3%	13.3%	13.3%	0%	13.3%	0%	6.7%	0%	0%	0%	0%	13.3%	0%	0%	0%	

Table 7: **Generalist Anomaly Detection** (\uparrow). We train TOTEM & GPT2 on all datasets and then perform in-domain and zero-shot evaluations. **A. In-Domain Performance.** TOTEM outperforms GPT2: **80.0%** vs. 20.0%. **B. Zero-Shot Performance.** TOTEM again outperforms GPT2: **73.3%** vs. 26.7%.

A. In-Domain Performance				B. Zero-Shot Performance			
Model		TOTEM	GPT2	Model		TOTEM	GPT2
F1	SMD	78.64	79.73	F1	N2	51.29	39.02
	MSL	83.29	80.17		N5	51.28	42.19
	SMAP	92.51	67.05		R	49.39	36.14
	SWAT	94.37	89.62		P	49.15	20.81
	PSM	95.78	90.47		S	52.17	38.12
R	SMD	72.07	73.42	R	N2	76.88	33.69
	MSL	82.96	78.48		N5	76.84	36.77
	SMAP	87.48	73.45		R	70.49	39.66
	SWAT	96.13	87.53		P	73.71	17.67
	PSM	93.90	87.76		S	77.36	31.83
P	SMD	86.66	87.44	P	N2	38.49	46.43
	MSL	83.64	81.95		N5	38.48	49.38
	SMAP	93.56	90.01		R	38.02	46.30
	SWAT	92.68	91.83		B	36.86	25.33
	PSM	97.74	93.39		S	39.35	47.72
AvgWins		80.0%	20.0%	AvgWins		73.3%	26.7%

Table 8: **Means & Stds. for the Anomaly Detection Task.** A. is the TOTEM specialist, B. is the TOTEM generalist, C. is the GPT2 generalist which we setup to run in a generalist manner.

A. TOTEM - Specialist Anomaly Detection (\uparrow)		B. TOTEM - Generalist Anomaly Detection (\uparrow)		C. GPT2 - Generalist Anomaly Detection (\uparrow)		
Mean \pm Std		Mean \pm Std		Mean \pm Std		
F1	SMD	0.7962 \pm 0.0137	SMD	0.7864 \pm 0.0386	SMD	0.7973 \pm 0.0326
	MSL	0.8258 \pm 0.0052	MSL	0.8329 \pm 0.0020	MSL	0.8017 \pm 0.0205
	SMAP	0.9402 \pm 0.0008	SMAP	0.9251 \pm 0.0014	SMAP	0.6705 \pm 0.0041
	SWAT	0.9427 \pm 0.0006	SWAT	0.9437 \pm 0.0005	SWAT	0.8962 \pm 0.0016
	PSM	0.9587 \pm 0.0008	PSM	0.9578 \pm 0.0002	PSM	0.9047 \pm 0.0759
R	N2	0.5129 \pm 0.0397	N2	0.5129 \pm 0.0397	N2	0.3902 \pm 0.0596
	N5	0.5128 \pm 0.0390	N5	0.5128 \pm 0.0390	N5	0.4219 \pm 0.0047
	R	0.4939 \pm 0.0625	R	0.4939 \pm 0.0625	R	0.3614 \pm 0.0204
	B	0.4915 \pm 0.0229	B	0.4915 \pm 0.0229	B	0.2081 \pm 0.0462
	S	0.5217 \pm 0.0418	S	0.5217 \pm 0.0418	S	0.3812 \pm 0.0621
P	SMD	0.7207 \pm 0.0565	SMD	0.7207 \pm 0.0565	SMD	0.7342 \pm 0.0559
	MSL	0.8296 \pm 0.0046	MSL	0.8296 \pm 0.0046	MSL	0.7848 \pm 0.0277
	SMAP	0.9148 \pm 0.0020	SMAP	0.9148 \pm 0.0020	SMAP	0.5342 \pm 0.0051
	SWAT	0.9613 \pm 0.0010	SWAT	0.9613 \pm 0.0010	SWAT	0.8753 \pm 0.0033
	PSM	0.9390 \pm 0.0004	PSM	0.9390 \pm 0.0004	PSM	0.8776 \pm 0.0624
P	N2	0.7688 \pm 0.0594	N2	0.7688 \pm 0.0594	N2	0.3369 \pm 0.0592
	N5	0.7684 \pm 0.0582	N5	0.7684 \pm 0.0582	N5	0.3677 \pm 0.0498
	R	0.7049 \pm 0.0825	R	0.7049 \pm 0.0825	R	0.2966 \pm 0.0218
	B	0.7371 \pm 0.0340	B	0.7371 \pm 0.0340	B	0.1767 \pm 0.0426
	S	0.7736 \pm 0.0581	S	0.7736 \pm 0.0581	S	0.3183 \pm 0.0648
P	SMD	0.8666 \pm 0.0114	SMD	0.8666 \pm 0.0114	SMD	0.8744 \pm 0.0029
	MSL	0.8364 \pm 0.0014	MSL	0.8364 \pm 0.0014	MSL	0.8195 \pm 0.0130
	SMAP	0.9356 \pm 0.0009	SMAP	0.9356 \pm 0.0009	SMAP	0.9001 \pm 0.0007
	SWAT	0.9268 \pm 0.0001	SWAT	0.9268 \pm 0.0001	SWAT	0.9183 \pm 0.0006
	PSM	0.9774 \pm 0.0002	PSM	0.9774 \pm 0.0002	PSM	0.9339 \pm 0.0925
P	N2	0.3849 \pm 0.0299	N2	0.3849 \pm 0.0299	N2	0.4643 \pm 0.0561
	N5	0.3848 \pm 0.0294	N5	0.3848 \pm 0.0294	N5	0.4958 \pm 0.0396
	R	0.3802 \pm 0.0502	R	0.3802 \pm 0.0502	R	0.4630 \pm 0.0139
	B	0.3686 \pm 0.0172	B	0.3686 \pm 0.0172	B	0.2533 \pm 0.0498
	S	0.3935 \pm 0.0325	S	0.3935 \pm 0.0325	S	0.4772 \pm 0.5000

Table 9: **Extra Anomaly Detection** (\uparrow). We present the the Adj. F1 metric the table (higher is better), then calculate the **AvgWins** . The selection criteria for the 15 datasets from (Wu & Keogh, 2021; Goswami et al., 2024) was the following. First, based only on the names in (Goswami et al., 2024), it was often ambiguous which data file was used. In these cases, we excluded the dataset. Second, we had difficulty verifying whether the default train/val/test ratios specified in the (Goswami et al., 2024) code matched what was reported. We found for the majority of datasets that the defaults resulted in test sets with no anomalies, when anomalies should be present. These were also excluded. From the results we could obtain, TOTEM matches or beats all other methods.

Model	TOTEM	ATran	MNT-0	MNT-LP	DGHL	GPT2	TiNet
CIMIS44AirTemperature3	73.8	6.0	100.0	98.0	50.0	18.0	47.0
GP711MarkerLFM5z4	96.7	76.0	69.0	97.0	31.0	48.0	90.0
InternalBleeding5	100.0	94.0	100.0	100.0	100.0	92.0	100.0
MesoplodonDensirostris	99.4	100.0	91.0	84.0	79.0	100.0	100.0
TKeepSecondMARS	100.0	83.0	95.0	100.0	16.0	12.0	95.0
WalkingAcceleration5	100.0	99.0	100.0	100.0	91.0	87.0	93.0
insectEPG2	100.0	12.0	11.0	23.0	14.0	81.0	96.0
ltstdbs30791AS	100.0	100.0	100.0	100.0	100.0	100.0	100.0
park3m	67.2	15.0	56.0	64.0	20.0	63.0	93.0
s20101mML2	100.0	69.0	65.0	71.0	15.0	5.0	8.0
sddb49	99.8	89.0	100.0	100.0	88.0	94.0	100.0
sel840mECG1	99.5	16.0	61.0	66.0	28.0	21.0	36.0
sel840mECG2	86.8	15.0	36.0	39.0	32.0	28.0	21.0
tiltAPB2	68.5	92.0	96.0	98.0	36.0	83.0	38.0
tiltAPB3	23.4	17.0	48.0	85.0	3.0	5.0	9.0
AvgWins	53.5%	13.3%	33.3%	53.5%	13.3%	13.3%	33.3%
Avg. Best Adj. F1	87.7	58.9	75.2	81.7	46.9	55.8	68.4

Table 12: **Means and Stds. for the Forecasting Specialists.** A. is the TOTEM specialist, B. is the GPT2 specialist which we setup to run with a consistent lookback.

A. TOTEM - Specialist Forecasting (\downarrow)				B. GPT2 - Specialist Forecasting, Lookback of 96 (\downarrow)			
Metric	MSE	Mean \pm Std		Metric	MSE	Mean \pm Std	
		MAE	MAE			MAE	MAE
W	96	0.165 \pm 0.0015	0.208 \pm 0.0012	96	0.184 \pm 0.0013	0.224 \pm 0.0014	
	192	0.207 \pm 0.0006	0.250 \pm 0.0012	192	0.233 \pm 0.0012	0.263 \pm 0.0009	
	336	0.257 \pm 0.0009	0.291 \pm 0.0006	336	0.285 \pm 0.0015	0.302 \pm 0.0013	
E	96	0.178 \pm 0.0015	0.263 \pm 0.0010	96	0.186 \pm 0.0004	0.272 \pm 0.0005	
	192	0.187 \pm 0.0015	0.273 \pm 0.0015	192	0.190 \pm 0.0007	0.278 \pm 0.0008	
	336	0.199 \pm 0.0012	0.285 \pm 0.0012	336	0.204 \pm 0.0003	0.291 \pm 0.0005	
T	96	0.523 \pm 0.0010	0.303 \pm 0.0006	96	0.471 \pm 0.0016	0.311 \pm 0.0016	
	192	0.530 \pm 0.0030	0.303 \pm 0.0017	192	0.479 \pm 0.0017	0.312 \pm 0.0010	
	336	0.549 \pm 0.0017	0.311 \pm 0.0021	336	0.490 \pm 0.0009	0.337 \pm 0.0010	
m1	96	0.320 \pm 0.0006	0.347 \pm 0.0006	96	0.328 \pm 0.0022	0.363 \pm 0.0014	
	192	0.379 \pm 0.0017	0.382 \pm 0.0012	192	0.386 \pm 0.0006	0.402 \pm 0.0006	
	336	0.406 \pm 0.0017	0.392 \pm 0.0026	336	0.400 \pm 0.0013	0.404 \pm 0.0011	
m2	96	0.176 \pm 0.0006	0.253 \pm 0.0010	96	0.178 \pm 0.0000	0.263 \pm 0.0000	
	192	0.247 \pm 0.0012	0.302 \pm 0.0015	192	0.245 \pm 0.0000	0.307 \pm 0.0000	
	336	0.317 \pm 0.0046	0.348 \pm 0.0031	336	0.307 \pm 0.0000	0.346 \pm 0.0000	
h1	96	0.380 \pm 0.0006	0.394 \pm 0.0000	96	0.379 \pm 0.0032	0.397 \pm 0.0007	
	192	0.434 \pm 0.0010	0.427 \pm 0.0006	192	0.438 \pm 0.0037	0.427 \pm 0.0004	
	336	0.490 \pm 0.0023	0.459 \pm 0.0015	336	0.474 \pm 0.0045	0.448 \pm 0.0053	
h2	96	0.293 \pm 0.0015	0.338 \pm 0.0006	96	0.293 \pm 0.0000	0.345 \pm 0.0000	
	192	0.375 \pm 0.0031	0.390 \pm 0.0026	192	0.318 \pm 0.0000	0.432 \pm 0.0000	
	336	0.431 \pm 0.0049	0.403 \pm 0.0031	336	0.418 \pm 0.0000	0.432 \pm 0.0000	
	720	0.610 \pm 0.0095	0.567 \pm 0.0081	720	0.423 \pm 0.0000	0.446 \pm 0.0000	

Table 13: **Means and Stds. for the Forecasting Generalist.** A. is the TOTEM generalist, B. is the GPT2 generalist which we setup to run in a generalist manner.

A. TOTEM - Generalist and Zero-Shot Forecasting (\downarrow)				B. GPT2 - Generalist and Zero-Shot Forecasting (\downarrow)			
Metric	MSE	Mean \pm Std		Metric	MSE	Mean \pm Std	
		MAE	MAE			MAE	MAE
W	96	0.172 \pm 0.0010	0.246 \pm 0.0006	96	0.204 \pm 0.0017	0.237 \pm 0.0012	
	192	0.217 \pm 0.0009	0.282 \pm 0.0006	192	0.230 \pm 0.0020	0.263 \pm 0.0006	
	336	0.266 \pm 0.0015	0.295 \pm 0.0012	336	0.298 \pm 0.0006	0.311 \pm 0.0006	
E	96	0.179 \pm 0.0006	0.264 \pm 0.0012	96	0.194 \pm 0.0012	0.278 \pm 0.0021	
	192	0.183 \pm 0.0006	0.264 \pm 0.0009	192	0.190 \pm 0.0006	0.278 \pm 0.0006	
	336	0.196 \pm 0.0020	0.283 \pm 0.0015	336	0.214 \pm 0.0012	0.300 \pm 0.0015	
T	96	0.507 \pm 0.0020	0.284 \pm 0.0006	96	0.484 \pm 0.0046	0.320 \pm 0.0042	
	192	0.511 \pm 0.0030	0.282 \pm 0.0006	192	0.488 \pm 0.0006	0.320 \pm 0.0006	
	336	0.535 \pm 0.0076	0.292 \pm 0.0012	336	0.502 \pm 0.0020	0.326 \pm 0.0021	
m1	96	0.374 \pm 0.0000	0.384 \pm 0.0006	96	0.487 \pm 0.0106	0.468 \pm 0.0035	
	192	0.400 \pm 0.0015	0.399 \pm 0.0023	192	0.516 \pm 0.0071	0.480 \pm 0.0021	
	336	0.432 \pm 0.0040	0.425 \pm 0.0015	336	0.418 \pm 0.0015	0.439 \pm 0.0013	
m2	96	0.198 \pm 0.0006	0.275 \pm 0.0012	96	0.243 \pm 0.0021	0.315 \pm 0.0021	
	192	0.266 \pm 0.0035	0.319 \pm 0.0021	192	0.297 \pm 0.0012	0.346 \pm 0.0010	
	336	0.336 \pm 0.0035	0.339 \pm 0.0025	336	0.319 \pm 0.0025	0.350 \pm 0.0020	
h1	96	0.382 \pm 0.0364	0.404 \pm 0.0012	96	0.421 \pm 0.0058	0.408 \pm 0.0010	
	192	0.463 \pm 0.0025	0.435 \pm 0.0006	192	0.480 \pm 0.0026	0.436 \pm 0.0020	
	336	0.507 \pm 0.0070	0.460 \pm 0.0019	336	0.512 \pm 0.0061	0.462 \pm 0.0052	
h2	96	0.307 \pm 0.0012	0.345 \pm 0.0015	96	0.298 \pm 0.0090	0.343 \pm 0.0049	
	192	0.406 \pm 0.0058	0.403 \pm 0.0023	192	0.381 \pm 0.0153	0.392 \pm 0.0072	
	336	0.505 \pm 0.0114	0.460 \pm 0.0035	336	0.406 \pm 0.0271	0.419 \pm 0.0144	
	720	0.601 \pm 0.0511	0.557 \pm 0.0215	720	0.423 \pm 0.0078	0.438 \pm 0.0051	
Zero-Shot				Zero-Shot			
N2	96	1.138 \pm 0.0032	0.777 \pm 0.0012	96	1.332 \pm 0.0012	0.830 \pm 0.0010	
	192	1.149 \pm 0.0011	0.785 \pm 0.0011	192	1.116 \pm 0.0081	0.863 \pm 0.0023	
	336	1.092 \pm 0.0062	0.770 \pm 0.0026	336	1.358 \pm 0.0123	0.851 \pm 0.0042	
N5	96	0.483 \pm 0.0012	0.484 \pm 0.0012	96	0.528 \pm 0.0006	0.499 \pm 0.0010	
	192	0.495 \pm 0.0021	0.491 \pm 0.0015	192	0.578 \pm 0.0015	0.524 \pm 0.0009	
	336	0.488 \pm 0.0031	0.483 \pm 0.0029	336	0.498 \pm 0.0046	0.495 \pm 0.0013	
R	96	1.120 \pm 0.0081	0.582 \pm 0.0036	96	1.465 \pm 0.0185	0.725 \pm 0.0031	
	192	1.242 \pm 0.0151	0.635 \pm 0.0074	192	1.638 \pm 0.0280	0.785 \pm 0.0078	
	336	0.488 \pm 0.0038	0.626 \pm 0.0076	336	0.792 \pm 0.0104	0.769 \pm 0.0060	
B	96	0.805 \pm 0.0070	0.739 \pm 0.0035	96	0.838 \pm 0.0149	0.762 \pm 0.0071	
	192	0.836 \pm 0.0040	0.752 \pm 0.0021	192	0.837 \pm 0.0095	0.732 \pm 0.0040	
	336	0.809 \pm 0.0038	0.748 \pm 0.0021	336	0.92 \pm 0.0066	0.738 \pm 0.0050	
S	96	0.446 \pm 0.0032	0.482 \pm 0.0017	96	0.443 \pm 0.0010	0.478 \pm 0.0006	
	192	0.462 \pm 0.0015	0.491 \pm 0.0010	192	0.481 \pm 0.0006	0.499 \pm 0.0006	
	336	0.521 \pm 0.0122	0.525 \pm 0.0068	336	0.523 \pm 0.0010	0.523 \pm 0.0006	
	720	0.717 \pm 0.0096	0.625 \pm 0.0040	720	0.743 \pm 0.0020	0.643 \pm 0.0010	

Metric	Tin \rightarrow Tout	Train	Test	TOTEM (Ours)	GPT2	TiNet	Patch	DLin	Re	Inf	Auto	Fed	LiTS
sMAPE	24 \rightarrow 18	M4-M	M3-M	14.4	14.1	14.0	14.7	15.7	14.8	15.9	16.9	15.1	24.6
sMAPE	48 \rightarrow 24	M3-M	M4-M	14.6	14.6	16.2	14.7	14.8	15.6	23.5	25.1	18.2	15.2
MAPE	12 \rightarrow 4	M4-Y	Tour.-Y	31.8	27.2	35.6	33.2	39.6	33.9	41.2	51.2	43.4	138.2
NDx100!	30 \rightarrow 168	M4-H	Elec.-H	17.6	17.2	19.3	17.3	17.6	21.6	21.2	33.9	18.4	19.6

Table 14: Short term forecasting results (lower is better). We randomly choose settings across varying input-to-output dimensionalites, train and test datasets, and find that TOTEM (Ours) and GPT2 outperform all other methods.

Table 15: **Long term vs. short term forecasting lookback and lookahead lengths.** We see that long term forecasting is far more stereotyped, and therefore easier to build generalist models for, than short term forecasting.

Dataset	Input → Output
Long Term Forecasting; In-Domain Testing	
All Datasets (enforced by us, Liu et al. (2023); Wu et al. (2022a); Liu et al. (2022b); Zhou et al. (2022))	96 → 96, 192, 336, 720
Long Term Forecasting; Zero Shot Testing	
All Datasets	96 → 96, 192, 336, 720
Short Term Forecasting; In Domain Testing	
M4-Y	12 → 6
M4-Q	16 → 8
M4-M	36 → 18
M4-W	26 → 13
M4-D	28 → 14
M4-H	96 → 48
Short Term Forecasting; Zero Shot Testing	
M4-Y, M3-Y	12 → 6
M4-Q, M3-Q	24 → 8
M4-M, M3-M	24 → 18
M4-M, M3-O	16 → 8
M3-Q, M4-Q	16 → 8
M3-M, M4-M	48 → 24
M3-Y, M4-Y	9 → 6
M3-M, M4-W	65 → 13
M3-M, M4-D	9 → 14
M3-O, M4-H	2 → 48
M4-Y, Tour-Y	12 → 4
M4-Q, Tour-Q	24 → 8
M4-M, Tour-M	36 → 24
M4-H, Elec-H	30 → 168

*Y=Yearly, Q=Quarterly, M=Monthly, W=Weekly, D=Daily, H=Hourly, O=Other

Table 16: **96 and 512 Lookback Lengths.** We compare various forecasters with a lookback length of 96 and 512, across all lookback lengths and datasets TOTEM has the most **AvgWins** at 58.3% followed by GPT2 at 8.3%.

Tin=512	Model	TOTEM (Ours)	GPT2	MNT	Patch	N-Beats
	Run By	TOTEM (Ours)	TOTEM (Ours)	N/A	Trans	N/A
Dataset	Metric	MSE, MAE	MSE, MAE	MSE, MAE	MSE, MAE	MSE, MAE
W	96	0.147, 0.196	0.162, 0.212	0.154, 0.209	0.149, 0.198	0.152, 0.210
W	192	0.195, 0.242	0.204, 0.248	N/A, N/A	0.194, 0.241	N/A, N/A
W	336	0.248, 0.283	0.254, 0.286	N/A, N/A	0.245, 0.282	N/A, N/A
W	720	0.314, 0.330	0.326, 0.337	0.315, 0.336	0.314, 0.334	0.331, 0.359
E	96	0.135, 0.231	0.139, 0.238	0.138, 0.242	0.129, 0.222	0.131, 0.228
E	192	0.151, 0.245	0.153, 0.251	N/A, N/A	0.147, 0.240	N/A, N/A
E	336	0.168, 0.265	0.169, 0.266	N/A, N/A	0.163, 0.259	N/A, N/A
E	720	0.200, 0.292	0.206, 0.297	0.211, 0.305	0.197, 0.290	0.208, 0.298
T	96	0.369, 0.241	0.388, 0.282	0.391, 0.282	0.360, 0.249	0.375, 0.259
T	192	0.383, 0.242	0.407, 0.290	N/A, N/A	0.379, 0.256	N/A, N/A
T	336	0.397, 0.248	0.412, 0.294	N/A, N/A	0.392, 0.264	N/A, N/A
T	720	0.446, 0.275	0.450, 0.312	0.450, 0.310	0.431, 0.286	0.508, 0.335
Tin=96	Model	TOTEM (Ours)	GPT2	MNT	Patch	N-Beats
	Run By	TOTEM (Ours)	TOTEM (Ours)	N/A	Trans	N/A
W	96	0.165, 0.208	0.184, 0.224	N/A, N/A	0.177, 0.218	N/A, N/A
W	192	0.207, 0.250	0.231, 0.263	N/A, N/A	0.225, 0.259	N/A, N/A
W	336	0.257, 0.291	0.285, 0.302	N/A, N/A	0.278, 0.297	N/A, N/A
W	720	0.326, 0.340	0.362, 0.351	N/A, N/A	0.354, 0.348	N/A, N/A
E	96	0.178, 0.263	0.186, 0.272	N/A, N/A	0.195, 0.285	N/A, N/A
E	192	0.187, 0.272	0.190, 0.278	N/A, N/A	0.199, 0.289	N/A, N/A
E	336	0.199, 0.285	0.204, 0.291	N/A, N/A	0.215, 0.305	N/A, N/A
E	720	0.236, 0.318	0.245, 0.324	N/A, N/A	0.256, 0.337	N/A, N/A
T	96	0.523, 0.303	0.471, 0.311	N/A, N/A	0.544, 0.359	N/A, N/A
T	192	0.530, 0.303	0.479, 0.312	N/A, N/A	0.540, 0.354	N/A, N/A
T	336	0.549, 0.311	0.490, 0.317	N/A, N/A	0.551, 0.358	N/A, N/A
T	720	0.598, 0.331	0.524, 0.336	N/A, N/A	0.586, 0.375	N/A, N/A
	AvgWins	58.3%	8.3%	0%	35.4%	0%

A.5 Ablation Details.

Table 17: **Ablations** (\downarrow). Across the Tokens vs. Time (TvT) experiments tokens out perform time. (A) specialist: 67.9% to 39.3%, (B) in-domain generalist: 78.6% to 23.2% , and (C) zero-shot generalist: 67.5% to 35%. (D) As the codebook size K increases the VQVAE reconstruction performance improves.

A. TvT Specialist					
Model	Metric	TOTEM		TimeTOTEM	
		MSE	MAE	MSE	MAE
W	96	0.165	0.208	0.164	0.209
	192	0.207	0.250	0.209	0.251
	336	0.257	0.291	0.261	0.293
	720	0.326	0.340	0.332	0.340
E	96	0.178	0.263	0.179	0.262
	192	0.187	0.272	0.185	0.269
	336	0.199	0.285	0.204	0.289
	720	0.236	0.318	0.244	0.325
T	96	0.523	0.303	0.528	0.310
	192	0.530	0.303	0.500	0.349
	336	0.549	0.311	0.531	0.365
	720	0.598	0.351	0.578	0.398
m1	96	0.320	0.347	0.326	0.355
	192	0.379	0.362	0.377	0.386
	336	0.406	0.402	0.409	0.409
	720	0.471	0.438	0.469	0.441
m2	96	0.176	0.253	0.176	0.254
	192	0.247	0.270	0.247	0.304
	336	0.317	0.348	0.318	0.350
	720	0.426	0.410	0.419	0.411
h1	96	0.380	0.394	0.377	0.395
	192	0.381	0.382	0.428	0.395
	336	0.490	0.459	0.480	0.462
	720	0.539	0.513	0.530	0.522
h2	96	0.293	0.338	0.294	0.338
	192	0.375	0.390	0.373	0.389
	336	0.422	0.431	0.423	0.433
	720	0.610	0.567	0.591	0.556
AvgWins		67.9%		39.3%	

B. TvT In-Domain Generalist					
Model	Metric	TOTEM		TimeTOTEM	
		MSE	MAE	MSE	MAE
W	96	0.172	0.216	0.173	0.218
	192	0.217	0.256	0.218	0.261
	336	0.266	0.295	0.267	0.299
	720	0.334	0.342	0.337	0.347
E	96	0.179	0.264	0.183	0.267
	192	0.181	0.267	0.189	0.275
	336	0.196	0.283	0.204	0.291
	720	0.230	0.314	0.242	0.325
T	96	0.507	0.284	0.517	0.293
	192	0.511	0.282	0.526	0.306
	336	0.535	0.292	0.552	0.304
	720	0.580	0.309	0.602	0.326
m1	96	0.374	0.384	0.428	0.420
	192	0.400	0.399	0.438	0.427
	336	0.432	0.424	0.469	0.447
	720	0.487	0.460	0.546	0.493
m2	96	0.198	0.275	0.207	0.286
	192	0.266	0.312	0.269	0.304
	336	0.365	0.342	0.358	0.377
	720	0.588	0.511	0.521	0.482
h1	96	0.382	0.404	0.401	0.410
	192	0.463	0.435	0.453	0.441
	336	0.507	0.463	0.496	0.468
	720	0.517	0.500	0.518	0.510
h2	96	0.307	0.345	0.305	0.346
	192	0.406	0.403	0.396	0.402
	336	0.505	0.460	0.492	0.458
	720	0.661	0.557	0.599	0.531
AvgWins		78.6%		23.2%	

C. TvT Zero-Shot Generalist					
Model	Metric	TOTEM		TimeTOTEM	
		MSE	MAE	MSE	MAE
N2	96	1.138	0.777	1.127	0.773
	192	1.149	0.785	1.169	0.793
	336	1.092	0.770	1.115	0.780
	720	1.045	0.754	1.070	0.766
N5	96	0.483	0.484	0.481	0.483
	192	0.495	0.491	0.508	0.500
	336	0.468	0.483	0.481	0.491
	720	0.451	0.477	0.467	0.488
R	96	1.120	0.582	1.102	0.578
	192	1.242	0.635	1.207	0.628
	336	1.237	0.626	1.190	0.613
	720	1.182	0.604	1.149	0.596
B	96	0.805	0.739	0.825	0.751
	192	0.836	0.752	0.847	0.761
	336	0.809	0.748	0.831	0.764
	720	0.896	0.794	0.928	0.813
S	96	0.446	0.482	0.446	0.481
	192	0.462	0.491	0.478	0.499
	336	0.521	0.525	0.535	0.532
	720	0.717	0.625	0.736	0.631
AvgWins		67.5%		35.0%	

D. Codebook Size Ablations				
Model	Metric	Codebook Size K		
		32	256	512
MSE				
All	0.0451	0.0192	0.0184	
T	0.0312	0.0120	0.0101	
E	0.0463	0.0209	0.0152	
W	0.0393	0.0161	0.0128	
MAE				
All	0.1460	0.0937	0.0913	
T	0.1204	0.0749	0.0685	
E	0.1520	0.1027	0.0878	
W	0.1122	0.0673	0.0607	
AvgWins		0%	0%	100%

E. TvT MLP Specialist					
Model	Metric	TOTEM		TimeTOTEM	
		MSE	MAE	MSE	MAE
W	96	0.164	0.210	0.180	0.224
	192	0.207	0.259	0.212	0.254
	336	0.259	0.293	0.273	0.302
	720	0.330	0.342	0.345	0.350
E	96	0.183	0.268	0.186	0.265
	192	0.188	0.275	0.190	0.271
	336	0.203	0.290	0.203	0.285
	720	0.240	0.323	0.240	0.319
T	96	0.539	0.330	0.556	0.332
	192	0.551	0.332	0.567	0.326
	336	0.565	0.336	0.577	0.329
	720	0.608	0.354	0.622	0.351
m1	96	0.332	0.362	0.335	0.368
	192	0.379	0.390	0.382	0.404
	336	0.418	0.423	0.421	0.421
	720	0.466	0.454	0.470	0.456
m2	96	0.178	0.257	0.179	0.259
	192	0.253	0.307	0.258	0.313
	336	0.336	0.361	0.333	0.359
	720	0.475	0.423	0.467	0.426
h1	96	0.391	0.409	0.407	0.419
	192	0.493	0.441	0.481	0.446
	336	0.642	0.506	0.541	0.468
	720	0.679	0.523	0.727	0.572
h2	96	0.362	0.368	0.326	0.353
	192	0.438	0.410	0.436	0.411
	336	0.543	0.457	0.922	0.670
	720	1.007	0.614	0.824	0.577
AvgWins		66.1%		37.5%	

Table 18: Mean & Stds. for the PatchTOTEM Ablation. Left is the specialist, right is the generalist.

Specialist Forecasting				Generalist In Domain & Zero Shot Forecasting			
	Metric	Mean \pm Std		MSE	Mean \pm Std		
		MSE	MAE		MSE	MAE	
W	96	0.164	\pm 0.0006	0.173	\pm 0.0012	0.218	\pm 0.0006
	192	0.209	\pm 0.0017	0.218	\pm 0.0006	0.261	\pm 0.0006
	336	0.261	\pm 0.0012	0.267	\pm 0.0006	0.299	\pm 0.0006
	720	0.332	\pm 0.0023	0.337	\pm 0.0010	0.347	\pm 0.0006
E	96	0.179	\pm 0.0015	0.183	\pm 0.0012	0.267	\pm 0.0012
	192	0.185	\pm 0.0006	0.183	\pm 0.0006	0.275	\pm 0.0006
	336	0.204	\pm 0.0055	0.204	\pm 0.0010	0.291	\pm 0.0010
	720	0.244	\pm 0.0040	0.243	\pm 0.0006	0.325	\pm 0.0006
T	96	0.326	\pm 0.0006	0.517	\pm 0.0000	0.293	\pm 0.0029
	192	0.500	\pm 0.0606	0.526	\pm 0.0030	0.296	\pm 0.0006
	336	0.531	\pm 0.0424	0.552	\pm 0.0015	0.304	\pm 0.0015
	720	0.578	\pm 0.0361	0.602	\pm 0.0046	0.326	\pm 0.0015
m1	96	0.326	\pm 0.0006	0.428	\pm 0.0090	0.420	\pm 0.0040
	192	0.377	\pm 0.0023	0.438	\pm 0.0015	0.427	\pm 0.0010
	336	0.409	\pm 0.0006	0.469	\pm 0.0062	0.447	\pm 0.0042
	720	0.469	\pm 0.0015	0.546	\pm 0.0081	0.493	\pm 0.0017
m2	96	0.377	\pm 0.0023	0.207	\pm 0.0015	0.286	\pm 0.0020
	192	0.480	\pm 0.0021	0.269	\pm 0.0015	0.325	\pm 0.0010
	336	0.480	\pm 0.0021	0.353	\pm 0.0199	0.377	\pm 0.0091
	720	0.530	\pm 0.0110	0.521	\pm 0.0165	0.482	\pm 0.0026
h1	96	0.294	\pm 0.0021	0.401	\pm 0.0006	0.410	\pm 0.0006
	192	0.373	\pm 0.0023	0.453	\pm 0.0010	0.441	\pm 0.0010
	336	0.423	\pm 0.0031	0.496	\pm 0.0017	0.468	\pm 0.0006
	720	0.591	\pm 0.0145	0.518	\pm 0.0020	0.510	\pm 0.0017
h2	96	0.294	\pm 0.0021	0.305	\pm 0.0006	0.346	\pm 0.0006
	192	0.373	\pm 0.0023	0.396	\pm 0.0015	0.402	\pm 0.0001
	336	0.423	\pm 0.0031	0.492	\pm 0.0310	0.458	\pm 0.0131
	720	0.591	\pm 0.0145	0.599	\pm 0.0105	0.531	\pm 0.0026
N2	96	0.377	\pm 0.0010	1.127	\pm 0.0017	0.773	\pm 0.0006
	192	0.428	\pm 0.0015	1.169	\pm 0.0032	0.793	\pm 0.0010
	336	0.480	\pm 0.0021	1.115	\pm 0.0010	0.780	\pm 0.0006
	720	0.530	\pm 0.0110	1.070	\pm 0.0035	0.766	\pm 0.0010
N5	96	0.294	\pm 0.0021	0.481	\pm 0.0015	0.483	\pm 0.0006
	192	0.373	\pm 0.0023	0.508	\pm 0.0012	0.500	\pm 0.0000
	336	0.423	\pm 0.0031	0.481	\pm 0.0006	0.491	\pm 0.0006
	720	0.591	\pm 0.0145	0.467	\pm 0.0010	0.488	\pm 0.0010
R	96	0.294	\pm 0.0021	1.102	\pm 0.0031	0.578	\pm 0.0021
	192	0.373	\pm 0.0023	1.207	\pm 0.0036	0.628	\pm 0.0017
	336	0.423	\pm 0.0031	1.190	\pm 0.0021	0.613	\pm 0.0010
	720	0.591	\pm 0.0145	1.149	\pm 0.0017	0.596	\pm 0.0020
B	96	0.294	\pm 0.0021	0.825	\pm 0.0079	0.751	\pm 0.0076
	192	0.373	\pm 0.0023	0.847	\pm 0.0021	0.761	\pm 0.0012
	336	0.423	\pm 0.0031	0.831	\pm 0.0066	0.764	\pm 0.0042
	720	0.591	\pm 0.0145	0.928	\pm 0.0131	0.813	\pm 0.0050
S	96	0.294	\pm 0.0021	0.446	\pm 0.0015	0.481	\pm 0.0010
	192	0.373	\pm 0.0023	0.478	\pm 0.0015	0.499	\pm 0.0000
	336	0.423	\pm 0.0031	0.535	\pm 0.0012	0.532	\pm 0.0006
	720	0.591	\pm 0.0145	0.736	\pm 0.0025	0.631	\pm 0.0006

Table 19: Mean and Stds. for the Codebook Ablation (\downarrow)

	K	Mean \pm Std	
		MSE	MAE
All	32	0.0451 \pm 0.0014	0.1460 \pm 0.0030
	256	0.0192 \pm 0.0003	0.0937 \pm 0.0007
	512	0.0184 \pm 0.0025	0.0913 \pm 0.0062
W	32	0.0393 \pm 0.0005	0.1122 \pm 0.0064
	256	0.0161 \pm 0.0004	0.0673 \pm 0.0011
	512	0.0128 \pm 0.0011	0.0607 \pm 0.0032
E	32	0.0463 \pm 0.0007	0.1520 \pm 0.0016
	256	0.0209 \pm 0.0012	0.1027 \pm 0.0029
	512	0.0152 \pm 0.0005	0.0878 \pm 0.0014
T	32	0.0312 \pm 0.0007	0.1204 \pm 0.0008
	256	0.0120 \pm 0.0003	0.0749 \pm 0.0007
	512	0.0101 \pm 0.0012	0.0685 \pm 0.0044

A.6 Further Exploration Details.

Table 20: Generalist codes beat specialist codes: 66.1% vs 57.1%.

Codebook Forecaster	Metric	Specialist Specialist		Generalist Specialist		Generalist Generalist	
		MSE	MAE	MSE	MAE	MSE	MAE
W	96	0.165	0.208	0.164	0.208	0.172	0.216
	192	0.207	0.250	0.208	0.251	0.217	0.256
	336	0.257	0.291	0.258	0.290	0.266	0.295
	720	0.326	0.340	0.329	0.338	0.334	0.342
E	96	0.178	0.263	0.178	0.263	0.179	0.264
	192	0.187	0.272	0.187	0.273	0.181	0.267
	336	0.199	0.265	0.199	0.265	0.196	0.283
	720	0.236	0.318	0.238	0.320	0.230	0.314
T	96	0.523	0.303	0.521	0.301	0.507	0.284
	192	0.530	0.303	0.530	0.303	0.511	0.282
	336	0.543	0.311	0.539	0.313	0.535	0.292
	720	0.598	0.331	0.605	0.337	0.580	0.309
m1	96	0.320	0.347	0.328	0.352	0.374	0.384
	192	0.379	0.382	0.377	0.383	0.400	0.399
	336	0.406	0.402	0.408	0.404	0.432	0.424
	720	0.471	0.438	0.470	0.440	0.487	0.460
m2	96	0.176	0.253	0.175	0.253	0.198	0.275
	192	0.247	0.302	0.247	0.302	0.266	0.319
	336	0.317	0.348	0.318	0.348	0.365	0.377
	720	0.426	0.410	0.427	0.410	0.588	0.511
h1	96	0.380	0.394	0.382	0.395	0.382	0.404
	192	0.434	0.427	0.437	0.427	0.463	0.435
	336	0.490	0.459	0.490	0.460	0.507	0.463
	720	0.539	0.513	0.536	0.512	0.517	0.500
h2	96	0.293	0.338	0.294	0.339	0.307	0.345
	192	0.375	0.390	0.375	0.391	0.406	0.403
	336	0.422	0.431	0.421	0.431	0.505	0.460
	720	0.610	0.567	0.610	0.567	0.661	0.557
AvgWins		57.1%		66.1%			

Table 21: Zero Shot Vignette: Training Size & Diversity

Model	Train Domain	Sensor Num (S)	Raw Length (T)	Train Size	TOTEM Generalist		TOTEM Specialist		TOTEM Specialist	
					MSE	MAE	MSE	MAE	MSE	MAE
N2	ALL	-	-	17.6M			Traffic		Electricity	
	96	-	-	10.2M			862		321	
	192	-	-	5.8M			17544		26304	
	336	-	-							
720										
N5	96									
	192									
	336									
	720									
R	96									
	192									
	336									
	720									
B	96									
	192									
	336									
	720									
S	96									
	192									
	336									
	720									
AvgWins		85.0%		2.5%		12.5%				

Table 22: Means and Stds. Mixed Models - Forecasting (↓)

Metric	Mean \pm Std		
	MSE	MAE	
W	96	0.164 \pm 0.0010	0.208 \pm 0.0012
	192	0.208 \pm 0.0010	0.251 \pm 0.0015
	336	0.258 \pm 0.0012	0.290 \pm 0.0015
	720	0.329 \pm 0.0021	0.338 \pm 0.0015
E	96	0.178 \pm 0.0006	0.263 \pm 0.0010
	192	0.187 \pm 0.0021	0.273 \pm 0.0017
	336	0.199 \pm 0.0012	0.283 \pm 0.0017
	720	0.238 \pm 0.0012	0.320 \pm 0.0012
T	96	0.521 \pm 0.0010	0.301 \pm 0.0010
	192	0.530 \pm 0.0023	0.303 \pm 0.0012
	336	0.555 \pm 0.0080	0.313 \pm 0.0072
	720	0.605 \pm 0.0097	0.337 \pm 0.0075
m1	96	0.328 \pm 0.0036	0.352 \pm 0.0006
	192	0.377 \pm 0.0021	0.383 \pm 0.0012
	336	0.408 \pm 0.0035	0.404 \pm 0.0021
	720	0.470 \pm 0.0035	0.440 \pm 0.0021
m2	96	0.175 \pm 0.0006	0.253 \pm 0.0010
	192	0.247 \pm 0.0006	0.303 \pm 0.0010
	336	0.318 \pm 0.0006	0.348 \pm 0.0031
	720	0.427 \pm 0.0012	0.410 \pm 0.0067
h1	96	0.382 \pm 0.0025	0.395 \pm 0.0015
	192	0.437 \pm 0.0012	0.427 \pm 0.0006
	336	0.490 \pm 0.0015	0.460 \pm 0.0021
	720	0.536 \pm 0.0031	0.512 \pm 0.0032
h2	96	0.294 \pm 0.0010	0.339 \pm 0.0012
	192	0.375 \pm 0.0025	0.391 \pm 0.0023
	336	0.421 \pm 0.0050	0.431 \pm 0.0031
	720	0.610 \pm 0.0089	0.567 \pm 0.0075

Table 23: Mean and Stds. Traffic Only - Specialist Zero-Shot Performance (↓)

Metric	Mean \pm Std		
	MSE	MAE	
N2	96	1.194 \pm 0.0062	0.798 \pm 0.0020
	192	1.218 \pm 0.0074	0.808 \pm 0.0023
	336	1.190 \pm 0.0133	0.804 \pm 0.0052
	720	1.117 \pm 0.0137	0.784 \pm 0.0056
N5	96	0.515 \pm 0.0026	0.505 \pm 0.0012
	192	0.535 \pm 0.0051	0.514 \pm 0.0028
	336	0.524 \pm 0.0071	0.513 \pm 0.0030
	720	0.500 \pm 0.0064	0.507 \pm 0.0032
R	96	1.171 \pm 0.0023	0.635 \pm 0.0019
	192	1.273 \pm 0.0090	0.673 \pm 0.0042
	336	1.232 \pm 0.0055	0.653 \pm 0.0022
	720	1.198 \pm 0.0057	0.642 \pm 0.0041
B	96	0.812 \pm 0.0037	0.749 \pm 0.0025
	192	0.858 \pm 0.0025	0.767 \pm 0.0015
	336	0.836 \pm 0.0041	0.759 \pm 0.0030
	720	0.919 \pm 0.0063	0.803 \pm 0.0037
S	96	0.476 \pm 0.0012	0.508 \pm 0.0012
	192	0.511 \pm 0.0005	0.528 \pm 0.0005
	336	0.576 \pm 0.0024	0.568 \pm 0.0009
	720	0.795 \pm 0.0017	0.685 \pm 0.0012

Table 24: Means and stds. Electricity Only - Specialist Zero-Shot Performance (↓)

Metric	Mean \pm Std		
	MSE	MAE	
N2	96	1.193 \pm 0.0059	0.802 \pm 0.0020
	192	1.300 \pm 0.0016	0.845 \pm 0.0003
	336	1.260 \pm 0.0162	0.837 \pm 0.0055
	720	1.234 \pm 0.0054	0.832 \pm 0.0016
N5	96	0.489 \pm 0.0024	0.490 \pm 0.0011
	192	0.535 \pm 0.0073	0.527 \pm 0.0007
	336	0.538 \pm 0.0064	0.525 \pm 0.0033
	720	0.533 \pm 0.0010	0.527 \pm 0.0006
R	96	1.141 \pm 0.0056	0.579 \pm 0.0028
	192	1.297 \pm 0.0162	0.652 \pm 0.0079
	336	1.247 \pm 0.0108	0.628 \pm 0.0059
	720	1.236 \pm 0.0053	0.633 \pm 0.0070
B	96	0.820 \pm 0.0065	0.756 \pm 0.0034
	192	0.843 \pm 0.0042	0.759 \pm 0.0022
	336	0.791 \pm 0.0023	0.741 \pm 0.0019
	720	0.886 \pm 0.0059	0.790 \pm 0.0020
S	96	0.460 \pm 0.0017	0.487 \pm 0.0010
	192	0.505 \pm 0.0017	0.511 \pm 0.0008
	336	0.569 \pm 0.0020	0.545 \pm 0.0011
	720	0.764 \pm 0.0046	0.641 \pm 0.0014

A.7 Codebook Visualizations.

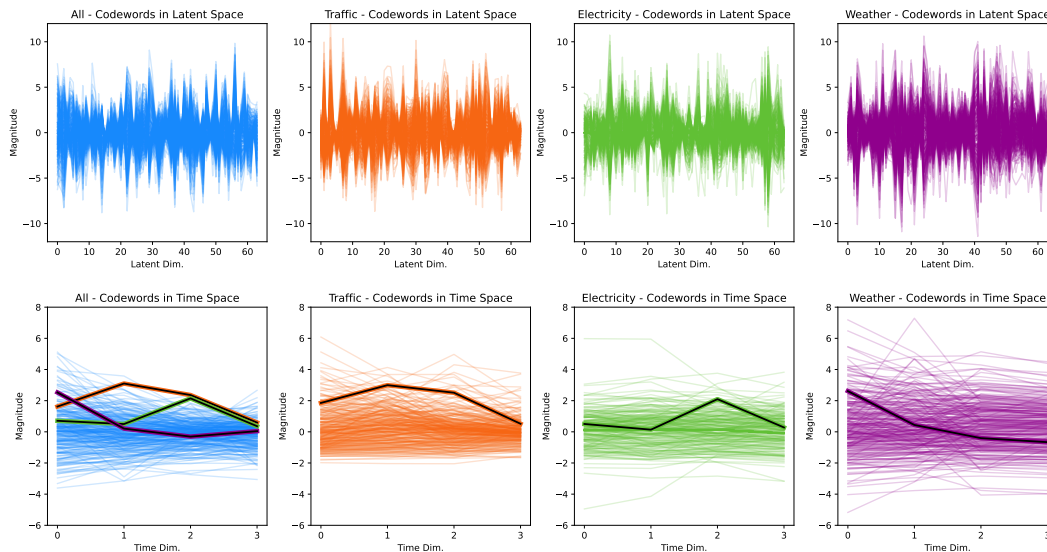


Figure 14: **TOTEM Codebooks**. We visualize all 256 codes for the generalist (All), and three specialists (Traffic, Electricity, and Weather). The top row visualizes codes in the latent space, the bottom row visualizes codes in the decoded time space. We additionally highlight codeword pairs matched via low MSE between All-Traffic, All-Electricity, and All-Weather in the bottom row.

A.8 TOTEM Examples.

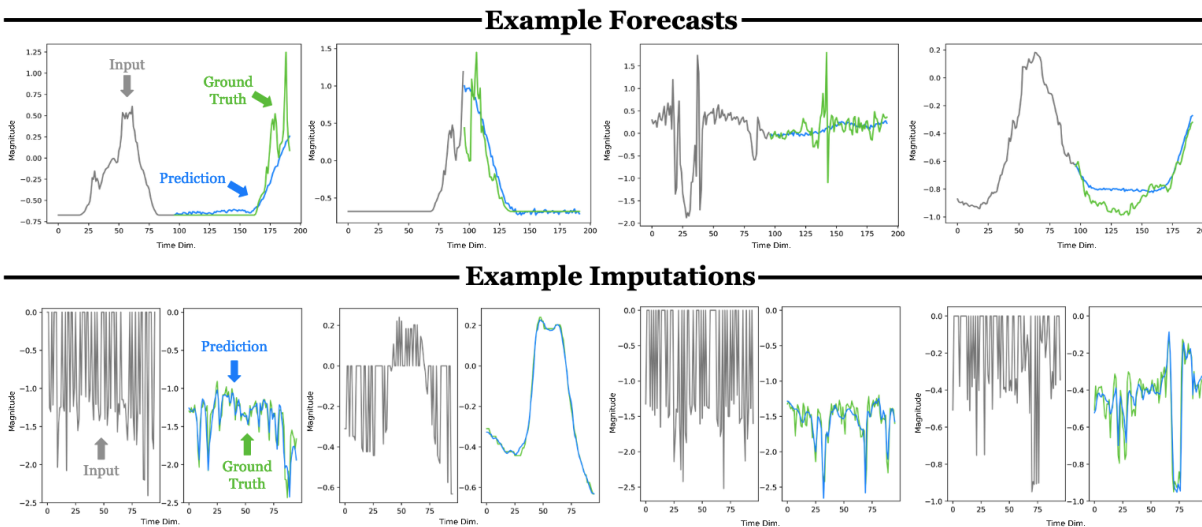


Figure 15: **TOTEM Examples**. In the top row we visualize four weather forecasts for $T_{in}=96$ and $T_{out}=96$. In the bottom row we visualize four ETTm2 imputations. In all cases the model input is in grey, the predictions are in blue, and the ground truth is in green.

A.9 Architecture Details.

VQVAE. For imputation, anomaly detection, and forecasting the VQVAE’s number of residual layers = 2, residual hidden size = 64, and block hidden size = 128 for all datasets. Each residual block has 2 non-causal, non-dilated 1D convolutional layers. The residual blocks are paired with additional non-causal, non-dilated 1D convolutional layers, where the number of additional layers is determined by the desired compression factor. See Table 25 for more hyperparameter details.

Table 25: **VQVAE Hyperparameters** (A) Imputation generalist (All) and specialists. (B) Anomaly detection generalist (All) and specialists. The anomaly %s for all of the zero shot datasets are 2%. (C) Forecasting generalist (All) and specialists.

A. Imputation.							B. Anomaly Detection.								
Dataset	LR	Iter.	BS	# CW	CW Dim.	CF	Dataset	LR	Iter.	BS	# CW	CW Dim.	CF	Anomaly %	
All	1e-3	120000	8192	512	64	4	All	1e-3	120000	4096	1024	64	4	Varies by test set.	
Elec.	1e-3	15000	8192	512	64	4	SMD	1e-3	60000	4096	1024	64	4		
Weather	1e-3	15000	8192	512	64	4	MSL	1e-3	15000	4096	1024	64	4		0.5
ETTm1	1e-3	15000	8192	512	64	4	PSM	1e-3	60000	4096	1024	64	4		1
ETTm2	1e-3	15000	8192	512	64	4	SMAP	1e-3	15000	4096	1024	64	4		1
ETTTh1	1e-3	15000	8192	512	64	4	SWAT	1e-3	15000	4096	1024	64	4		1
ETTTh2	1e-3	15000	8192	512	64	4									

C. Forecasting.						
Dataset	LR	Iter.	BS	# CW	CW Dim.	CF
All	1e-3	15000	4096	256	64	4
Elec.	1e-3	15000	4096	256	64	4
Weather	1e-3	15000	4096	256	64	4
Traffic	1e-3	15000	4096	256	64	4
ETTm1	1e-3	15000	4096	256	64	4
ETTm2	1e-3	15000	4096	256	64	4
ETTTh1	1e-3	15000	4096	256	64	4
ETTTh2	1e-3	15000	4096	256	64	4

Downstream Forecaster. The downstream forecaster has two components the transformer encoder that intakes codes and outputs a normalized time forecast, and the feedforward neural network that takes in time and outputs predictions for the forecast’s mean and standard deviation. The downstream forecaster is a transformer encoder with a model dimension = 64, hidden dimension = 256, number of heads = 4, number of layers = 4. The transformer encoder applies a sin / cos positional embedding along the time dimension and applies its attention mechanism to each sensor independently. There is a single linear layer applied after the transformer encoder output. The feedforward neural network takes in the input time steps, and predicts the future’s mean and standard deviation.

A.10 Training Details.

In imputation, anomaly detection, and forecasting the VQVAE is trained with a learning rate of 0.001 using the Adam optimizer, embedding dimension of 64, commitment cost of 0.25, and compression factor of 4; see Table 25 for more hyperparameters. The codewords are uniformly randomly initialized over $[\frac{-1}{K}, \frac{1}{K}]$, where K is the number of codewords and D is the latent dimension. In all tasks there is a global normalization, and local normalization Kim et al. (2021); both are standard throughout prior work. In imputation we only leverage global normalization, in anomaly detection and forecasting we utilize both global and local normalization. In anomaly detection we evaluate the models we run, TOTEM and GPT2, with both local normalized data and non-local normalized data for each method and report whichever schema leads to the best performance. In forecasting the downstream model is a transformer encoder with 4 layers and 4 attention heads and a feed-forward hidden dimension of 256. We train using Adam with a base learning rate of 0.0001 and a one cycle learning rate scheduler in accordance with Nie et al. (2022) on A100s.